POLYCAPROLACTONE MATRICES GENERATED IN AQUEOUS MEDIA: NATURAL POLYMERS IMMOBILIZATION AND STRESS RELAXATION BEHAVIOR

By

KORNKARN MAKORNKAEWKEYOON

Bachelor of Engineering in Chemical Engineering

Chulalongkorn University

Bangkok, Thailand

2007

Submitted to the Faculty of the
Graduate College of the
Oklahoma State University
in partial fulfillment of
the requirements for
the Degree of
MASTER OF SCIENCE
May, 2010

POLYCAPROLACTONE MATRICES GENERATED IN AQUEOUS MEDIA: NATURAL POLYMERS IMMOBILIZATION AND STRESS RELAXATION BEHAVIOR

Thesis Approved:

Dr. Sundararajan V. Madihally

Thesis Adviser

Dr. R. Russell Rhinehart

Dr. Josh Ramsey

Dr. A. Gordon Emslie

Dean of the Graduate College

ACKNOWLEDGMENTS

I would like to express my sincere gratitude to my advisor, Dr. Sundar Madihally, for all the guidance, suggestions, and encouragement he provided for my research. Having him as my advisor, I really had a good time working and learning throughout the time as a graduate student at OSU. I will do my best to make a good use of all the knowledge I learned from him in the future.

I would like to thank Dr.Russell R. Rhinehart and Dr.Josh Ramsey for being my committees and for all their help and support they gave me, especially in completing my thesis. I also would like to thank Eileen, Mindy, and Melissa for their help in administrative matters. I am really grateful to all my friends - Seok Won Pok, Rahul Mirani, Pooja Iyer, and Dhananjay Dhane for their help. Finally, I would like to thank Krisada Leemasawatdigul and Pongtorn Charoensuppanimit for their unconditional help and support throughout the time that we have known each other.

TABLE OF CONTENTS

Chapter **Page**

I. INTRODUCTION 1

II. BACKGROUND 6

Tissue Engineering 6
Natural Polymers 8
Synthetic Polymers 10
Polycaprolactone (PCL) 10
Mechanical Properties of Biomaterials 11
Tensile and Compressive Strength 11
Elastic Modulus 13
Viscoelasticity 13
Viscoelastic Models 14

III. IMMOBILIZATION OF NATURAL POLYMERS 19

Materials and Methods 20
Results 23
Immobilizing DS and gelatin onto PCL matrixes 23
Surface Characteristic and Sidedness Property of PCL Matrices 24
Attachment of Chitosan Porous Structure to PCL Matrices 26
Tensile properties 28
Discussion 32

Chapter **Page**

IV. STRESS RELAXATION BEHAVIOR 34

Materials and Methods 35
Model Development 37
Results 45
Effect of Applied Strain Rate to Stress Relaxation Behavior 45
Effect of Natural Polymers Immobilization to Stress Relaxation Behavior ... 47
Selection of the Most Appropriate Model 48
Discussion 55

V. CONCLUSIONS AND RECOMMENDATIONS 57

Conclusions 57
Recommendations 59

REFERENCES 61

LIST OF TABLES

Table **Page**

4.1 Average parameter values with standard deviations of 1AxB-3KxTau (Architecture A) with one hyperelastic and three linear spring-and-dashpot pseudo-components 50

4.2 Average parameter values with standard deviations of 3AxB-3Tau (Architecture B) with three retain pseudo-components 50

4.3 Average parameter values with standard deviations of 3AxB-2Tau (Architecture C) with different pseudo-component combinations 51

LIST OF FIGURES

Figure **Page**

2.1 Basic concept of tissue engineering 7

2.2 Raw materials for extracting gelatin 9

2.3 Stress-strain curve example of a ductile material 13

2.4 Stress-strain curve for a viscoelastic material 15

2.5 Schematic representation of (a) Maxwell model and (b) Kelvin–Voigt model 17

3.1 Schematic showing the sidedness of self-assembled PCL matrix 20

3.2 Toluidine blue staining of the matrix (a) Self assembled PCL without DS immobilization (b) Self assembled PCL after DS immobilization (c) chloroform-casted PCL without DS immobilization (d) chloroform-casted PCL after DS immobilization 23

3.3 Scanning electron micrographs of the top side of PCL matrices (a) self assembled PCL without DS immobilization, (b) self assembled PCL after DS immobilization, (c) self-assembled PCL after immobilization with gelatin, (d) chloroform-casted PCL 24

3.4 Scanning electron micrographs of the bottom side of PCL matrices (a) self-assembled PCL without DS immobilization, (b) self-assembled PCL after DS immobilization, (c) self-assembled PCL after immobilization with gelatin, (d) chloroform-casted PCL 25

3.5 Chitosan porous structure on PCL matrix (a) self-assembled PCL with gelatin and porous structure on the top side, (b) self-assembled PCL with gelatin and porous structure on the bottom side, (c) scanning electron micrographs showing porous structure, (d) detachment of chitosan matrix after 70% Ethanol treatment 26

Figure **Page**

3.6 Tensile stress-strain plot of PCL matrices (a) Dry condition, (b) Wet condition (c) initial slope (E1), (d) second slope (E2) 28

3.7 Tensile stress-strain plot of PCL matrices with chitosan matrix attached at the bottom side (a) dry condition, (b) wet condition, (c) elastic modulus (E1) of PCL with chitosan matrix formed on the bottom side 30

4.1 Concept of viscoelastic stress relaxation (a) material at rest (b) material elongated and stressed (c) material elongated and held while stress partially relaxes and (d) material released 37

4.2 Conceptual illustration of (a) the difference in material response after relaxation and (b) Instantaneous stress-strain relation 38

4.3 Model conceptual illustration (A) 1AxB-3KxTau (B) 3AxB-3Tau and (C) 3AxB-2Tau 42

4.4 Stress relaxation plot at different loading rate (a) 0.6%/s loading for 50 s and 100 s relaxation time (b) 1.0%/s loading for 30 s and 30 s relaxation time and (c) 3.0%/s loading for 10 s and 20 s relaxation time (d) stress accumulation of 0.6%/s strain rate (e) stress accumulation of 1.0%/s strain rate (f) stress accumulation of 3.0%/s strain rate 45

4.5 Relaxation function, G(t), plot from the characteristic trend of the first stage of each strain rate with the error bars represented the standard deviations from 5 tests 46

4.6 Stress relaxation of PCL matrices (a) Effect of multiple ramp-hold cycles, (b) Relaxation function, G(t), of PCL matrices 47

4.7 Comparison of each model fitting with the experimental data at 1% s^{-1} strain rate (A) 1AxB-3KxTau (B) 3AxB-3Tau and (C) 3AxB-2Tau 48

4.8 Comparison of Architecture C with each characteristic trial pseudo-component combination at 1% s^{-1} strain rate 52

CHAPTER I

INTRODUCTION

Tissue or organ failure is one of the most serious problems in human healthcare. Only in the U.S., millions of people suffer tissue loss or organ failure every year, which cost more than $400 billion per year [1]. The most common treatments currently used for tissue or organ loss are organ transplantation [2], surgical reconstruction [3], or using mechanical devices such as kidney dialyzers [4]. However, due to many limitations, these treatments are not the best solutions for the problems. Transplantation is still limited by donor shortage. As stated by the United Network for Organ Sharing (5 December 1996), 'the number one issue facing the transplant community is organ shortage'. Simply stated, there is one donor available for every 10 patients with a need for a transplanted organ. Surgical reconstruction can result in long-term problems such as chronic pain or discomfort [5]. Mechanical devices cannot perform all of the functions of an organ and are insufficient for the patient to fully recovered and live normally. For these reasons, the need for an alternative treatment for tissue or organ loss remains. With the attempt to provide solutions for such problems, the field of tissue engineering was developed.

The field of tissue engineering involves tissue or organ repair and replacement using the knowledge of engineering and life science in combination [1]. As an example of tissue engineering applications, the use of biodegradable materials as scaffolds for supporting cells is one promising solution for tissue regeneration. Both naturally formed matrices and synthetic matrices have been studied as scaffolds. Naturally formed matrices have the advantage of facilitating cell attachment and differentiation, but this group of materials has the problems of batch-to-batch variations and the difficulties of large batch production [6]. For this reason, synthetic matrices formed by biodegradable materials have been explored as scaffolds [7-11]. The advantage of a synthetic matrix is that its properties can be controlled more precisely, which make the production in large scale practical and reliable.

Many types of biodegradable materials have been studied in order to find the most suitable materials for forming scaffolds. Natural polymers, such as gelatin, chitosan, and glycosaminoglycans, are advantageous in supporting cell regulation, but their mechanical properties are difficult to match with human tissues as synthetic tissues. Many techniques have been suggested to solve the issue, such as blending natural polymers with synthetic polymers that have adjustable mechanical properties [11] or grafting natural polymers onto synthetic polymers[12]. Although these methods help improve the properties of the scaffolds for tissue regeneration, the cost and practicability in large scale of these complicated processes is still questionable.

The objective of this study was to gain better understanding of self-assembled polycaprolactone (PCL) - a unique solvent system (97% acetic acid) to dissolve PCL and form matrices by spontaneous precipitation in water [13], and its potential as a scaffold

for tissue engineering applications. Due to the hydrophilic nature of the polymer, the possibility as well as the effect of natural polymers immobilization onto self-assembled PCL was evaluated. The immobilization of natural polymers was tested because it may help improving cell regulation on PCL matrices. This study can be divided into two specific aims.

SPECIFIC AIM 1: Immobilization of Natural Polymers

Self-assembled PCL matrices were formed by dropping PCL solution onto water surface. Then, with the attempt to improve the bioregulatory activity of PCL matrices by natural polymers immobilization - attaching natural polymers onto the matrix surface, the following natural polymers were tested.

a) Dextran sulfate (DS), a glycosaminoglycan (GAGs) analogue, was one of the natural polymers used in this study to mimic the bioactivity of GAGs which have been shown to control cellular differentiation, migration, and proliferation.
b) Gelatin was used to mimic the bioactivity of collagen, which is known to promote cell activity.
c) Chitosan porous structure was incorporated with self-assemble PCL to make 3D structures for tissue regeneration.

The surface architecture of the matrices was analyzed by scanning electron microscopy (SEM) and, in order to understand the effect of natural polymer immobilization, constant-rate uniaxial tensile tests were performed under both in dry and wet conditions. Self-assembled PCL matrices exhibited different behavior between in dry and wet condition and the study showed that the immobilization of natural polymers

caused the elastic modulus to be higher, or the matrices to be stiffer. However, the differences were not statistically significant. These results showed the potential of self-assembled PCL matrices to be used for tissue regeneration. Our preliminary study also revealed another unique property of self-assembled PCL matrix. The PCL matrix formed by the self-assembly was found to have different surface architecture between two side of the matrix, which is called "sidedness property", due to the different surface in contact when the matrix was formed.

SPECIFIC AIM 2: Analysis of Stress Relaxation Behavior

Ramp-and-hold tests were performed to assess the stress relaxation properties of the scaffolds. The test consists of a loading phase where the sample is subjected to a constant rate of loading up to a specific value of percentage strain. The sample is then held at the specified strain for a period of time, which is the relaxation phase. There are four sections of analysis for this specific aim.

a) Effect of different strain rate on self-assembled PCL stress relaxation behavior was studied under three different sets of stress test treatments. The results show that there was little effect of strain rate in the range tested (0.1-3% s^{-1}) to the stress relaxation behavior since the differences were statistically insignificant.

b) Both plain and immobilized PCL matrices were tested to study the effect of immobilization on the stress relaxation behavior of self-assembled PCL matrices. The difference in stress relaxation behavior was not statistically significant, which indicates that the natural polymer immobilization did not alter the relaxation behavior of the PCL matrices.

c) Three composite models were tested to find the best fit model. Each model had different numbers of parameters and pseudo-components. Screening revealed that the architecture of 3 hyperelastic springs and 2 retain pseudo-components, which has 8 parameters, was the best model.

d) After the best composite model was selected, different combination of pseudo-components were tested. The combination that contained only spring-and-dashpot pseudo-components was the best fit. The combination of retain and return pseudo-components fit the self-assembled PCL experimental data. The benefit of this combination is that it provides a more realistic explanation for the mechanism than the spring-and-dashpot pseudo-component. However, the combination failed to fit well with chloroform-casted PCL data considered from the obtained sum of squared errors.

CHAPTER II

BACKGROUND

Tissue Engineering

The definition of "tissue engineering" was developed during the meeting held by the National Science Foundation (NSF) in 1988 at Lake Tahoe, California [14].

> "Tissue engineering" is the application of the principles and methods of engineering and the life sciences toward the fundamental understanding of structure/function relationships in normal and pathological mammalian tissues and the development of biological substitutes to restore, maintain, or improve functions."

From this definition, the essence of tissue engineering is to use the knowledge about cells, material and engineering in development of implantable parts or devices, which leads to the restoration or replacement of tissues or organ.

As an example of tissue engineering application, the basic approach of tissue regeneration is shown in **Figure 2.1**. One of the paths in repairing or replacement of tissues shown in the figure is using the scaffold to support the cells and placing it to the injury site. In order to make this tissue regeneration approach effective, selecting

materials that is suitable for the application is necessary. The minimum properties of the materials are biodegradability, biocompatibility and favorable interaction between cells. Biodegradability means that the scaffold material should eventually be able to biologically degrade and leave only normal healthy tissues to avoid the long-term complications [1, 15]. Biocompatibility means that the material and its degradation products should not be toxic or cause immune response in human body.

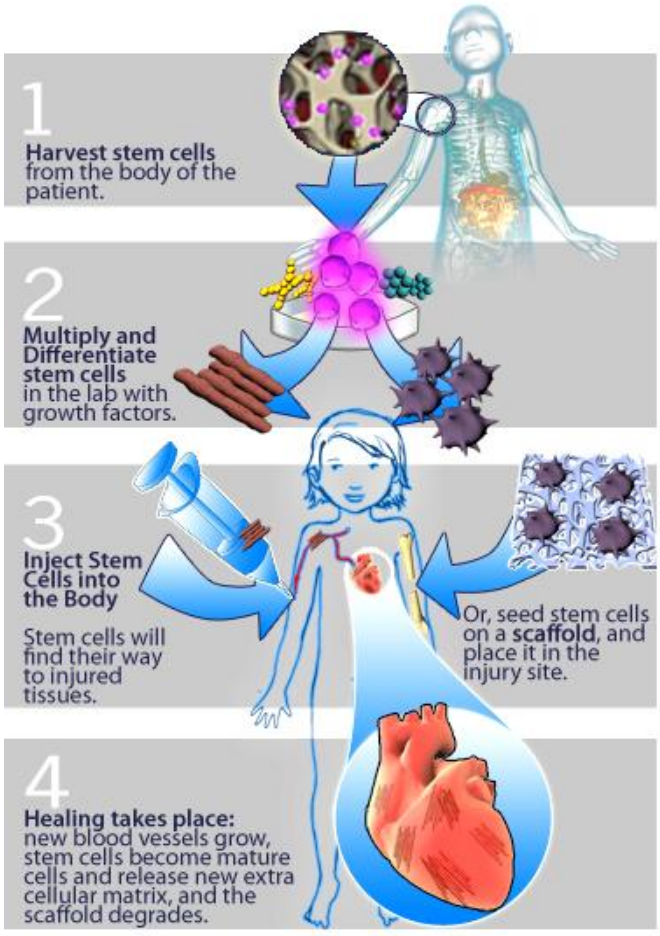

Figure 2.1. Basic concept of tissue engineering *(Picture from: http://www.duq.edu/sepa/regmed/regmedbasics/sepa_regmedbasics_regmedhealing.shtml)*

The scaffold must provide an environment suitable for cellular growth, and should contain suitable surface properties (porosity, wettability, stiffness, and compliance) to support cell attachment, proliferation, and differentiation. It is also important to select material with suitable mechanical properties; how materials respond when external force is applied in different patterns.

Of all the materials available, polymers are widely interested and explored as biomaterials, due to varieties and adjustability of properties. Polymers can be divided into two types based on the sources that they are derived; natural and synthetic polymers.

Natural Polymers

This group consists of naturally occurring polymers and chemical modifications of these polymers. These materials and their derivatives offer a wide range of properties and applications. Natural polymers are interested for tissue engineering applications due to its availability, biodegradability, biocompatibility and supporting cell regulation. However, natural polymers still have some drawbacks for the applications, which is the difficulty to tailor its mechanical properties. The examples of natural polymers currently used in tissue engineering applications and also in this research are gelatin, chitosan and glycosaminoglycans (GAGs) or its analogue, dextran sulfate.

Gelatin is a natural polymer derived from collagen, which can be extracted from skin, bones, and connective tissues of animals. It is composed of a unique sequence of amino acid and it has the ability to form gels when combined with water [16] and widely investigated for tissue engineering applications for years [9, 17-19].

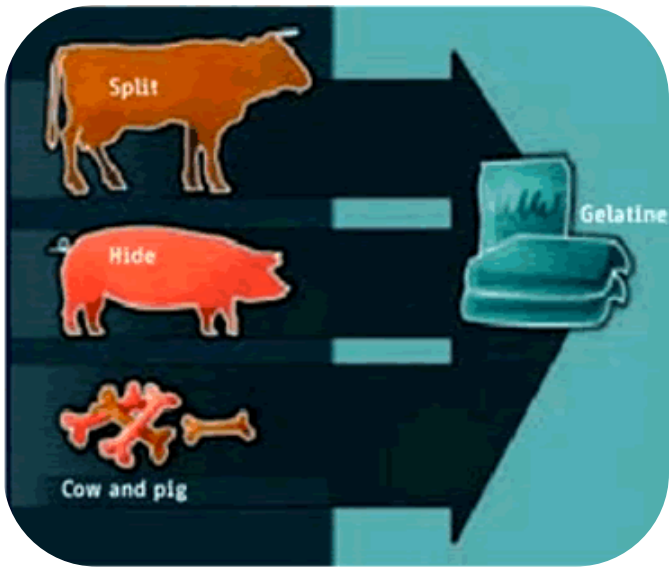

Figure 2.2. Raw materials for extracting gelatin *(Pictures from: http://www.geafiltration.com/library/gelatin_processing_aid.asp)*

Chitosan is produced by deacetylation of chitin, which is commonly found in shells of crustaceans (crabs, shrimps, etc.) and cell walls of fungi. Chitosan possesses two main interesting abilities that benefit its usage in tissue engineering. First, it has the ability to form porous structure by freezing and lyophilizing chitosan solution, which facilitates cell adhesion and colonization. Second, chitosan has anti-microbial activity function [20] which decreases the chance of infection at the injury site. However, chitosan becomes very rigid and brittle compared to soft tissue tissue (Young's modulus of spinal cord tissue was reported to be 0.2 – 0.8MPa while Young's modulus of chitosan is about 6MPa) and has a very low break strain (40-50%) [8], which are disadvantages for scaffolds used for tissue regeneration. Consequently, due to the anti-bacterial property, chitosan has been blended with other polymers to make scaffolds [21] to improve the polymers properties.

Glycosaminoglycans (GAGs) are groups of high molecular weight polysaccharides, which contain amino sugars and they are able to form complexes with protein. Dextran sulfate is a synthetic analogue of glycosaminoglyucans and derived from dextran. Dextran sulfate has been used as an anticoagulant and has shown to inhibit the replication of Human Immunodeficiency Virus (HIV) *in vitro* [22]. First, dextran was investigated as a blood plasma replacement [23] and has become of interest as a biodegradable and biocompatible material. It is able to be used for hydrogel formation, which is appealing for tissue engineering applications [24, 25].

Synthetic Polymers

Synthetic polymers are chemically manufactured from monomers with various functional groups. Synthetic biopolymers have played an important role in tissue engineering and have been explored extensively for decades [26, 27]. The advantages of this type of polymers are their adjustable mechanical, and degradation properties and easy processing. However, they do not possess necessary functional sequences that help in the regulation of biological activity. Hence, they have poor bioregulatory activity which is the major requirement for tissue engineering applications.

Polycaprolactone (PCL)

In particular, synthetic polyester polycaprolactone (PCL) [28, 29] has generated immense interest in various biomedical applications [30]. PCL is one of the most interested biopolymers due to its soft- and hard-tissue compatible properties [31]. PCL has good mechanical properties and low melting point (about 60°C) which helps

facilitating the processing of the material. Apart from low melting point (60°C) of PCL, ability to tailor its mechanical and non-enzymatic degradation (by hydrolysis) properties by altering MW are very attractive properties [32]; PCL membranes formed after dissolution in chloroform show elongation up to 1000% before break [33]. PCL degrades by hydrolysis (i.e., non-enzymatically). Their degradation rates and mechanical properties can be altered via co- and graft-polymerization techniques and processing conditions. However, the poor wettability of the matrices prevents uniform distribution of proteins and cell adhesion molecules, thus compromising the application of PCL as tissue engineering templates [34].

PCL matrixes also shows poor regulation on cellular activity [35], primarily due to the lack of cell adhesive proteins and hydrophobic nature. There has been some effort to improve these limitations by grafting RGD peptides (necessary for cellular attachment) [36, 37]. However, apart from RGD sequence necessary for cell adhesion, substrate has to mediate a variety of signals such as growth factor activity, cell migration and proliferation to regulate the biological response of diverse cell types.

Biological Tissues Characteristics

Different types of biological tissues display different characteristics, depending on the specific functions that those tissues perform. For example, the human skin, a nonlinear viscoelastic material, has a very low elastic coefficient (0.000057 MPa) and very flexible compared to other tissues of human body [38]. On the contrary, bone, which is a connective tissue subjected to constant compressive and shear stresses, has a much higher elastic coefficient (100 – 100,000 MPa) [38] and exhibit as a linear elastic

material [39, 40]. Heart, another important organ of human, contains different types of tissues that have different characteristics to perform the function normally. The first type is muscle tissue, which helps in pumping blood to and from the whole body. The second type is fibrous tissue for the heart valves and other special types that help maintaining the rate and regulating the rhythm of the beating [41]. Since each type of tissue has a unique characteristic, requirement for the material properties depends on the tissue type that the material is going to be used for.

Mechanical Properties of Biomaterials

It is important to understand mechanical properties of materials in order to choose a suitable material for each application. The material has to be able to support the stress as well as the local tissue that is replaced or repaired. Some mechanical properties that are often considered for tissue engineering applications are tensile and compressive strength and elastic modulus.

Tensile and Compressive Strength

Tensile strength is used for considering the material ability to withstand tension while compressive strength is used for considering the material ability to withstand compression. The tensile test is conducted by pulling a material sample using constant crosshead speed until the sample is broken. On the contrary, compressive test is conducted by applying a constant, uniaxial, compressive load until the sample is crushed. From the tests, tensile and compressive strengths are indicated by a stress-strain curve as

shown in **Figure 2.3**. Generally, tensile or compressive strength is the stress at which the material completely fails.

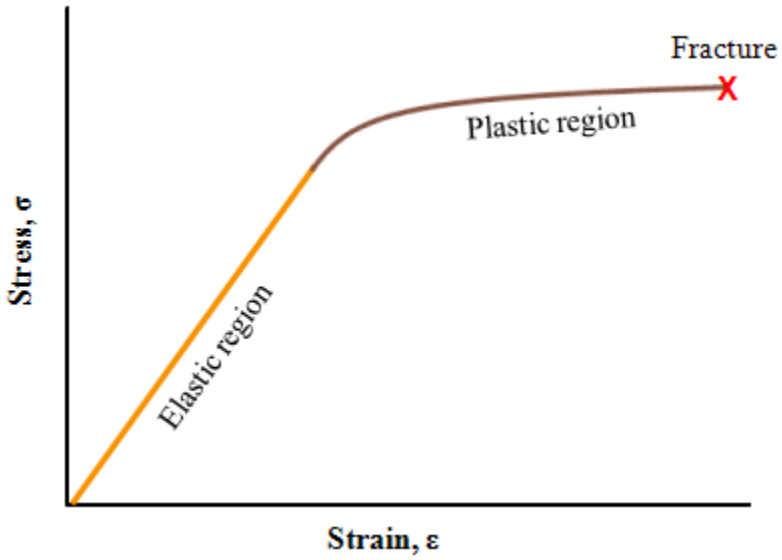

Figure 2.3. Stress-strain curve example of a ductile material

Typically, if a constant loading is applied to a material, two types of material deformation can be observed before it fails. The first type is elastic deformation which is reversible. The material returns to its original state if the loading is removed. The second type is plastic deformation. The material in the plastic deformation cannot return to its original state after the loading is removed.

Elastic Modulus

Elastic modulus describes the material's tendency to be deformed elastically along the axis that the force is applied. It is calculated from the slope of the stress-strain curve at the elastic region.

$$elastic\ modulus = \frac{stress}{strain}$$

The higher the value means more force is needed to make the material deform and the less flexible the material is.

Although these mechanical properties are able to be used as criteria of selecting a material for general purposes, they are insufficient for tissue engineering applications. It is more likely that the material will be exposed to small-magnitude loading in cyclical and sequential patterns than a long period of constant high-magnitude loading.

Viscoelasticity

Biological tissues display time-dependent and load-history-dependent mechanical behavior. A well-studied characteristic of human tissues, which is important for choosing materials to be used for tissue repairing or replacement, is viscoelasticity. These materials exhibit both viscous and elastic characteristics when exposed to external stresses or strains. Viscoelastic materials store and dissipate energy within complex molecular and multi-component structures; producing hysteresis (**Figure 2.4**) and allowing creep and stress relaxation to occur. The structure gradually returns toward its original state after the external stress or strain is removed.

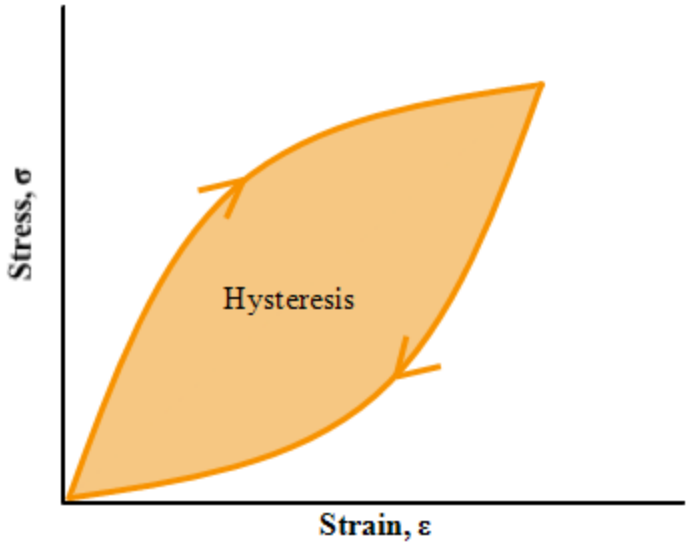

Figure 2.4. Stress-strain curve for a viscoelastic material

Viscoelasticity is a unique behavior observed in biological tissues. It is important to understand this behavior in order to choose the most suitable materials for tissue repairing or replacement. Accordingly, synthetic tissue structures for organ repair, and *in vitro* tissue structures for research purposes is better to possess the same viscoelastic mechanical properties as the native environment for the cell structures. The viscoelastic properties of tissues create an environment for cells which is critical for their viability and function. Although many studies about viscoelastic behavior of tissues are available [42-45], the information is insufficient for understanding the mechanisms of material performance needed for intelligent design of synthetic tissues.

Viscoelastic Models

Many viscoelastic models for describing the behavior of biomaterial have been proposed. Quasi-linear Viscoelastic (QLV) modeling approach, introduced by Fung in 1967 [46] and subsequently modified by many others, is the most utilized model in tissue

engineering literature of viscoelastic tissue models. The QLV theory assumes a separation of an instantaneous elastic response, $\sigma^e(\varepsilon)$, and a reduced relaxation function $G(t)$, for a step change in strain. The constitutive equation relating stress (σ) and strain (ε) for soft tissue stress relaxation behavior is given by the convolution integral:

$$\sigma(t) = G(t)^* \sigma^e(\varepsilon) \tag{1}$$

where "*" indicates the convolution integral expressed as

$$\sigma(t) = \int_0^t G(t-\tau) \frac{\partial \sigma^e(t)}{\partial \varepsilon} \frac{\partial \varepsilon}{\partial \tau} d\tau \tag{2}$$

For soft tissues, a generalized reduced relaxation function equation based on a continuous spectrum of relaxation was proposed as shown in Equation (3):

$$G(t) = \frac{1+C[E_1(t/\tau_2) - E_1(t/\tau_1)]}{1+C \ln \tau_2/\tau_1} \tag{3}$$

where C is a dimensionless material parameter that reflects the magnitude of viscous effects present and is related to the fraction of relaxation, τ_1 and τ_2 are time-constants that demark limits of the short and long-term material responses, and $E_1(t/\tau)$ is the exponential integral function of the form

$$E_1(t/\tau_2) = \int_{t/\tau}^{\infty} \frac{e^{-z}}{z} dz \tag{4}$$

QLV models, however, have several weaknesses, including: incapability to model nonlinear, nonstationary, and confounding aspects of biological tissues structures [10, 47-50]. Further, the parametric coefficients do not have a direct relation to either molecular structure or physical meaning.

Another complimentary modeling approach uses spring-and-dashpot based constitutive models, modified by including nonlinear hyperelastic "spring" elements.

The original model of the material undergoing strain is modeled with "spring" as restorative force component and "dashpot" as damping component.

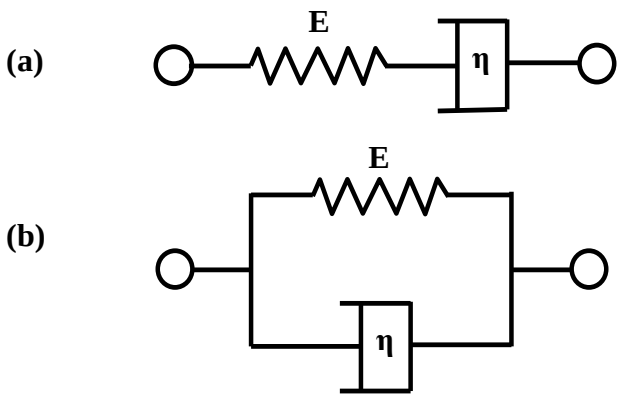

Figure 2.5. Schematic representation of (a) Maxwell model and (b) Kelvin–Voigt model

There are two types of models using this spring-and-dashpot element. The first one is called "Maxwell material" depicted by connecting a spring and dashpot in series. The relation of stress σ, and strain ε, is given by the equation below.

$$\frac{1}{E}\frac{d\sigma}{dt} + \frac{\sigma}{\eta} = \frac{d\varepsilon}{dt} \tag{5}$$

where E is the elastic modulus and η is the material coefficient of viscosity.

Another model using a spring and dashpot connecting in parallel is called "Kelvin–Voigt material". The constitutive equation relating stress σ, and strain ε is

$$\sigma(t) = E\varepsilon(t) + \eta\frac{d\varepsilon(t)}{dt} \tag{6}$$

Although both QLV and modified spring-and-dashpot constitutive models are effective, they lack physical relevance and do not reflect either the mechanistic understanding or phenomenological fidelity [51-53]. Hence, a better model that can predict the viscoelastic behavior of a material with supporting physical meanings is still needed.

CHAPTER III

IMMOBILIZATION OF NATURAL POLYMERS

A unique solvent system (97% acetic acid) to dissolve PCL and form matrices by spontaneous precipitation in water [13] is a new technique developed in our laboratory which is called “self-assembled”. Self-assembled PCL matrix is hydrophilic and water is able to uniformly distribute onto its surface, probably due to the miscibility of the solvent used. To better understand the effectiveness of generating matrices by self-assembly, the surface roughness characteristics was compared with the popular method of casting PCL matrices after dissolving in chloroform. AFM analyses of self-assembled matrices showed a significant increase in roughness relative to chloroform-casted matrices. Also, self-assembled matrixes in water had a net positive surface charge where as matrix formed by air drying chloroform based solution had a negative surface charge.

In this study, the possibility of natural polymer immobilization on PCL matrices was investigated. Immobilization of natural polymers helps improve cell adhesion on the surface of the synthetic polymers matrices. Dextran sulfate was one of the natural polymers used in this study to mimic the

bioactivity of glycosaminoglycans (GAGs) [54]; GAGs have been shown to control cellular differentiation, migration, and proliferation. Secondly, gelatin was used to mimic the bioactivity of collagen [13], which is known to promote cell adhesion. Since porous regions are necessary to grow three-dimensional tissues, forming Chitosan porous structure was also investigated with the intention of using the self-assembled matrixes in tissue regeneration. The surface architecture of the matrices was analyzed by scanning electron microscopy (SEM) and the tensile properties and the stress relaxation behavior were also investigated. These results showed the potential of self-assembled PCL matrices to be used for tissue regeneration.

Materials and methods

Sources of Material

Polycaprolactone of 47 kDa (Mn) was purchased from Polysciences (Warrington, PA). Low molecular weight Chitosan (50 kDa based on viscosity), type A porcine skin gelatin (approximately 300 bloom), 500 kDa DS (contains 0.5-2.0% phosphate buffer salts) and Toluidine Blue O (with 90% dye content, approximately) were obtained from Sigma Aldrich Chemical Co (St. Louis, MO). Glacial acetic acid was purchased from Pharmco Products Inc (Brookfield, CN). Pure ethanol was from AAPER (Shelbyville, KY).

Matrix Generation

First, 3-4 mL of 10% (wt/v) PCL solution prepared in glacial acetic acid, was gently dropped on the surface of water in an two inches in diameter Teflon dish and air

dried until the matrix was completely formed. The matrix was neutralized in ethanol for ten minutes and, then, washed with water. The side that did not touch the water when formed is referred as "top side" and other side is referred as "bottom side" (**Figure 3.1**). Since majority of the published studies use chloroform as a solvent, PCL matrices were formed by air drying 2 mL PCL solution (10% w/v) in chloroform and were also used to compare obtained results.

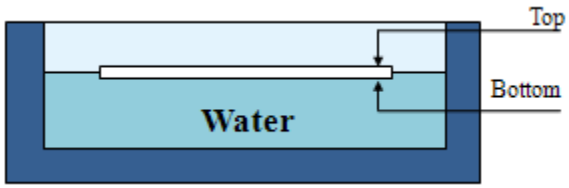

Figure 3.1. Schematic showing the sidedness of self assembled PCL matrix.

Immobilization of Dextran Sulfate (DS) and Gelatin

Freshly-made matrix (without ethanol neutralization) was incubated at room temperature in

i) 0.1% (wt/v) DS aqueous solution for ten minutes for immobilization of DS, or

ii) 1.0% (wt/v) gelatin solution for 30 minutes for immobilization of gelatin.

Then, both samples were washed with water.

The Identification of DS on the Matrix Surface

In order to test the presence of DS on the matrix, 0.075 mg/mL toluidine blue solution (prepared in an aqueous medium) was used. Seven to eight milliliters of the solution was added and allowed to react with the matrix for ten minutes.

Incorporating Chitosan Porous Structure

Chitosan solution (0.5% (w/v)) was prepared by mixing 0.5 g chitosan in 100 mL water with two milliliters of 10% (v/v) HCl aqueous solution added. The solution was stirred overnight for chitosan being completely dissolved. Four to five milliliters of 0.5% (wt/v) chitosan solution was dropped on the top side of a matrix and on the bottom side of another matrix. The samples were frozen at -20°C and lyophilized overnight.

Surface Analysis

For surface analysis of the PCL matrices, the dry samples were attached to aluminum stubs with carbon paint and sputter coated with gold for 40 seconds. Then, the surface architecture of the matrices was analyzed by scanning electron microscopy (SEM, JEOL USA Inc., Peabody, MA) at an accelerating voltage of 10 kV.

Tensile Test

From freshly prepared samples, 12 mm × 30 mm rectangular strip was cut and utilized for tensile testing in an INSTRON 5842 (INSTRON Inc., Canton, MA) mechanical testing machine at 10 mm/min, as described previously [11]. In brief, tests were performed at room temperature (25°C) for the dry condition and at 37°C for the wet condition (in phosphate-buffered saline (PBS) solution). Before performing the tensile test in wet condition, the samples were incubated in 100% ethanol for ten minutes before testing. The first and second elastic modulii were calculated from the slopes of the linear portion (0 - 3% tensile strain for the first elastic modulus and 40 – 90% tensile strain for the second elastic modulus) of the stress-strain curve.

To measure the thickness of the matrices, digital micrographs were obtained at various locations through an inverted microscope (Nikon TE2000U, Melville, NY) equipped with a CCD camera, as described previously. These images were quantified for the thickness using image analysis software Sigma Scan Pro (SPSS Science, Chicago, IL), calibrated using a micrograph of a hemocytometer at the same magnification. Four to five images were obtained per sample with at least ten points per image. The calculated minimum thicknesses were used for determining the stress values in each sample.

Results

Immobilizing DS and gelatin onto PCL matrixes

In presence of sulfate group, toluidine blue forms a purple color complex. PCL matrices incubated in DS solution showed purple stain while the matrices dipped in water had no purple stain (**Figure 3.2a** and **Figure 3.2b**). The appearance of purple color showed the presence of DS on self-assembled PCL matrices. One of the observations was that if all stained self-assembled matrices dried in air, both with and without DS, the color would change to purple. On the other hand, PCL matrixes formed in chloroform had no purple stain both with and without DS which mean there was no attachment of DS on the matrix surface (**Figure 3.2c** and **Figure 3.2d**). No purple color was observed in chloroform casted PCL matrixes.

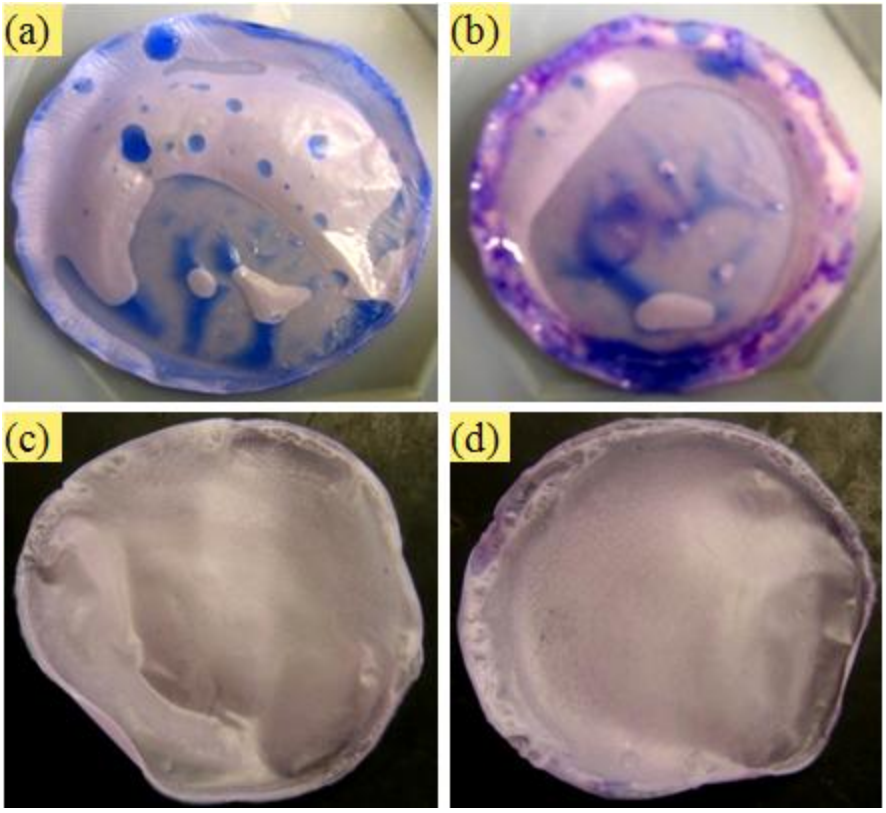

Figure 3.2. Toluidine blue staining of the matrix (a) Self assembled PCL without DS immobilization (b) Self assembled PCL after DS immobilization (c) chloroform-casted PCL without DS immobilization (d) chloroform-casted PCL after DS immobilization.

Surface Characteristic and Sidedness Property of PCL Matrices

In order to understand the changes in microarchitecture, the DS-immobilized membranes were analyzed via SEM. The matrix with immobilized DS (**Figure 3.3b**) showed less small size pores than one without DS immobilization, probably due to the presence of DS (**Figure 3.3a**). Similarly, the matrix with immobilized gelatin (**Figure 3.3c**) showed less small size pores than one without gelatin, similar to previous report, similar to previously results [13] and rougher surface than PCL matrixes with and without DS immobilization. Importantly, the top and bottom side of the self-assembled

PCL matrixes showed different characteristics; while the top side had porous structure, the bottom side had rough surface features without any pores (**Figure 3.4**). The DS-immobilized matrices had smoother surface than the plain and gelatin-immobilized matrices. However, both sides of all PCL matrices from the self-assembled method were much rougher than those from the chloroform-casted matrices (**Figure 3.3d** and **Figure 3.4d**).

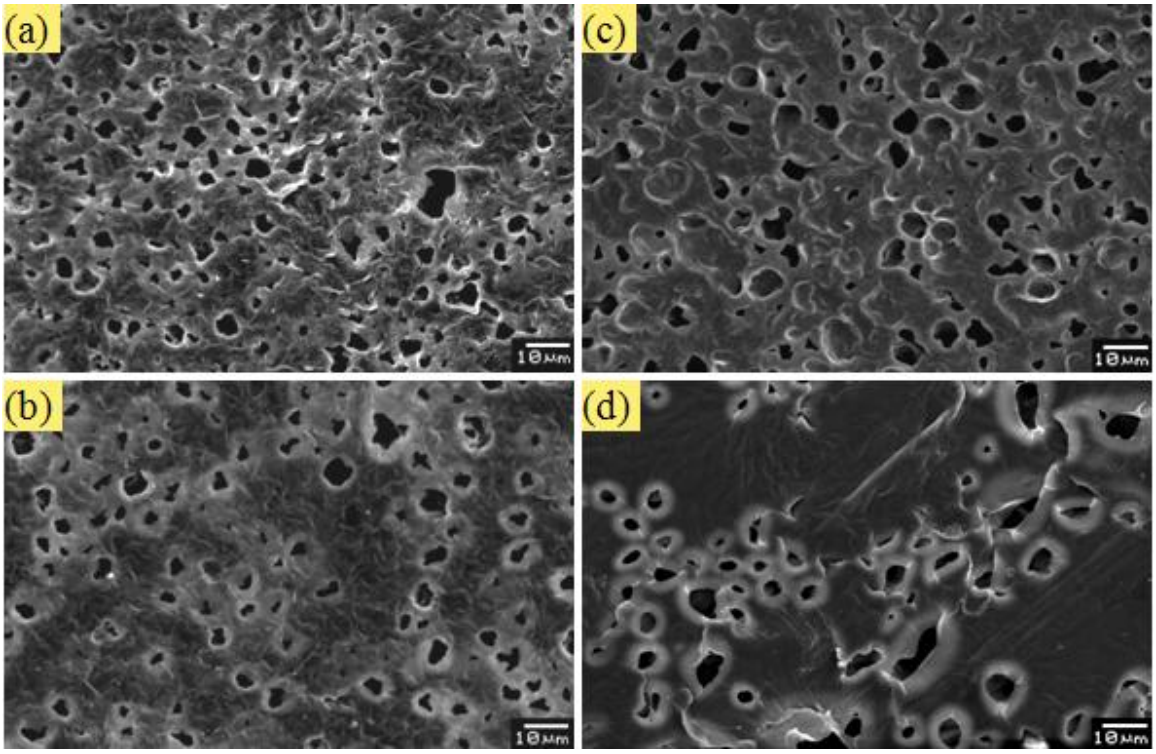

Figure 3.3. Scanning electron micrographs of the top side of PCL matrices (a) self assembled PCL without DS immobilization, (b) self assembled PCL after DS immobilization, (c) self-assembled PCL after immobilization with gelatin, (d) chloroform-casted PCL

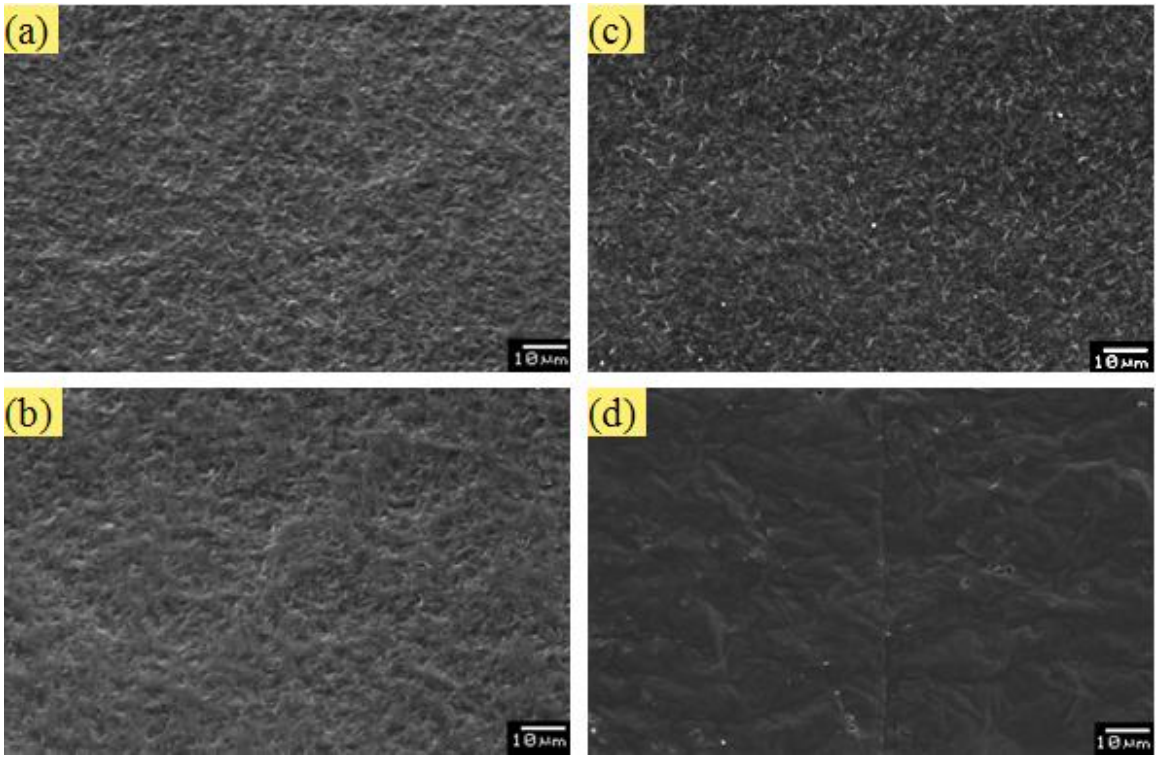

Figure 3.4. Scanning electron micrographs of the bottom side of PCL matrices (a) self-assembled PCL without DS immobilization, (b) self-assembled PCL after DS immobilization, (c) self-assembled PCL after immobilization with gelatin, (d) chloroform-casted PCL

Attachment of Chitosan Porous Structure to PCL Matrices

We questioned whether it is possible to directly attach chitosan porous structure to PCL without any additional treatment. These results showed that the chitosan porous structure formed by freeze drying could attach to the bottom side of the self-assembled PCL matrix better than the top side. Since chitosan complexes with negatively charged DS and gelatin, we also formed porous structures on PCL matrices incubated in DS and gelatin solution. However, there was no significant difference in the attachment of chitosan porous structure on PCL alone matrix and DS immobilized PCL matrix. On the

contrary, the binding of chitosan on PCL with immobilized gelatin was slightly stronger than both PCL alone and DS immobilized PCL matrices (**Figure 3.5a**).

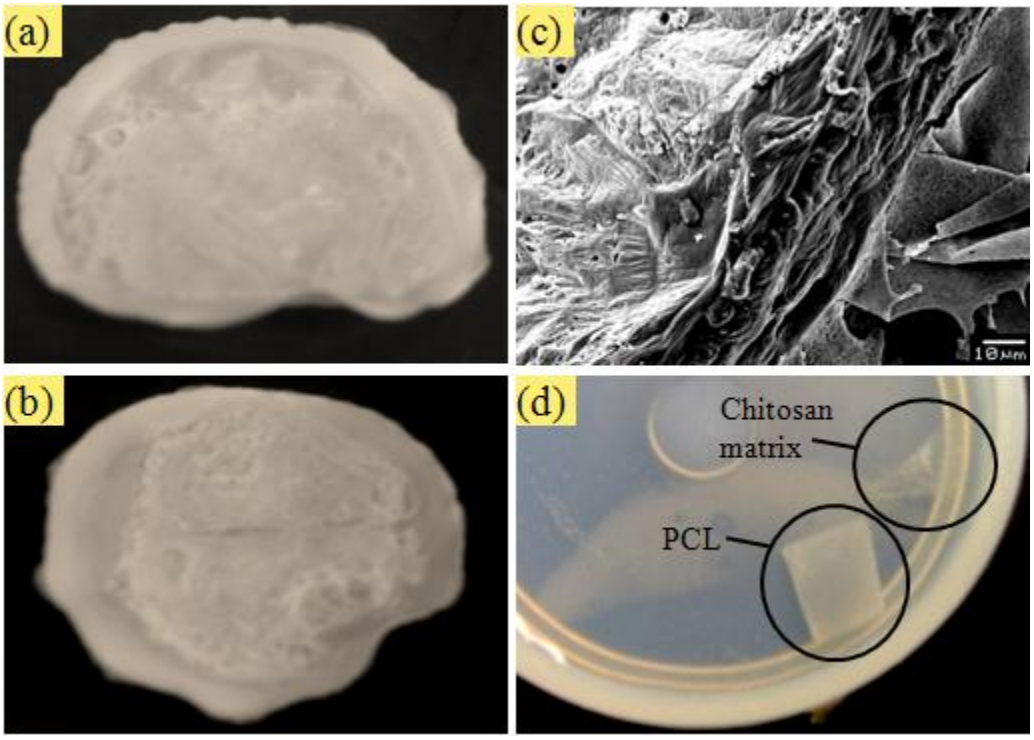

Figure 3.5. Chitosan porous structure on PCL matrix (a) self-assembled PCL with gelatin and porous structure on the top side, (b) self-assembled PCL with gelatin and porous structure on the bottom side, (c) scanning electron micrographs showing porous structure, (d) detachment of chitosan matrix after 70% Ethanol treatment

Since many of the biological applications need hydration, the samples were neutralized and hydrated with ethanol. During this time, the chitosan matrix detached from PCL matrix (**Figure 3.5d**). To test whether this is due to the absence of water which makes chitosan very brittle, three solutions containing water were used; 70% (v/v) ethanol, 0.1% (w/v) NaOH and PBS solution. Both 70% ethanol and 0.1% NaOH gave the same result that chitosan matrix easily came off from the PCL. For PBS solution, the

chitosan matrix turned into a gel but still attached to the PCL matrix. From all the obtained results, the tensile test in wet condition was performed on the PCL matrices after the chitosan matrix came off instead so that the change in properties from the effect of chitosan could be seen.

Tensile properties

When PCL matrixes were tested for tensile properties in dry condition at 25°C, all matrixes showed similar behavior (**Figure 3.6a**). In general chloroform casted matrixes showed higher stress level relative to acetic acid casted matrixes. Strain ranges were similar in all conditions. However, when the samples were tested in hydrated condition and at 37°C, there was a significant difference in the strain range between acetic acid casted matrixes to chloroform casted matrixes. Chloroform casted matrixes had a behavior similar to dry conditions with high stress levels and low strain ranges. On the contrary acetic acid casted matrixes had significantly increased strain range with decreased stress level.

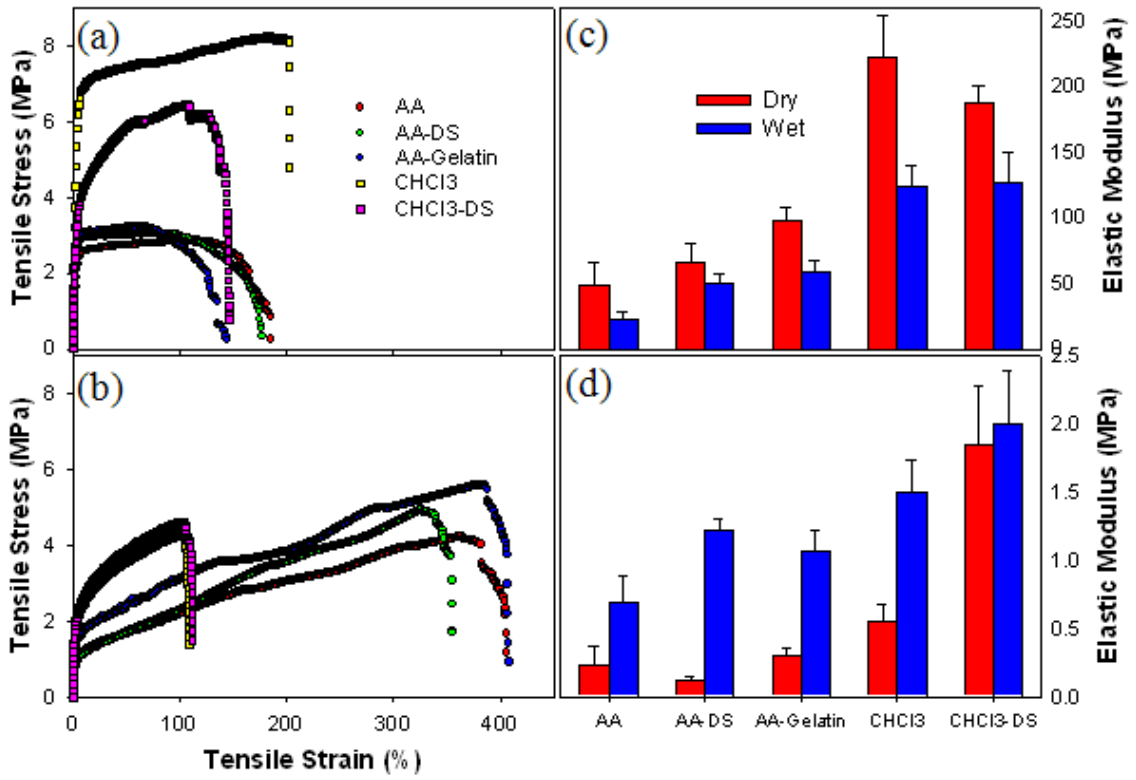

Figure 3.6. Tensile stress-strain plot of PCL matrices (a) Dry condition, (b) Wet condition (c) initial slope (E1), (d) second slope (E2) (AA – self-assembled PCL, AA-DS - self-assembled PCL with immobilized DS, AA-Gelatin - self-assembled PCL with immobilized gelatin, CHCl3 – chloroform-casted PCL, and CHCl3-DS – chloroform-casted PCL with immobilized DS)

To better understand the stress-strain behavior, the stress-strain response was classified into two regions: (i) elastic region showing a linear relationship between stress and strain; (ii) plastic region after the elastic sectin. The matrices tested in dry and wet conditions showed different characteristic in the plastic region. There was little change in tensile stress when tensile strain was increased in dry condition. In wet condition, the results showed the trend of linear behavior with different slopes from the first section. To better understand, the first modulus (E1) was calculated from the slope of the elastic

region (**Figure 3.6c**) and the second modulus (E2) was calculated from the slope of the plastic region (**Figure 3.6d**). The samples tested in dry condition had higher E1 than samples tested in wet condition, particularly self-assembled PCL matrixes. Chloroform-casted PCL matrices had much higher first elastic modulus than those of self-assembled PCL matrices in both wet and dry conditions. The trend of the results agreed with our previous study [13]. The matrices with immobilized DS had higher first elastic modulus than the PCL alone matrixes in both wet and dry conditions. The matrix with immobilized gelatin had the highest first elastic modulus in both dry and wet condition compared to the self-assembled PCL matrices. However, there was no statistically significant difference between immobilized DS and immobilized gelatin PCL matrixes in wet condition, unlike in dry condition. Although the break strain of all samples was not significantly different in dry condition, the break strain of the chloroform-casted sample was lower than that of the self-assembled matrixes in wet condition. This is opposite from that observed using 80 kDa PCL, reported previously [13]. Further, there was no initial surge in stress for chloroform-casted 47 kDa PCL matrixes. These differences could be attributed to the molecular weight. There was no significant change in second elastic modulus of PCL matrixes with immobilized DS and immobilized gelatin.

Tensile tests were also performed on PCL matrixes processed for attaching chitosan porous structure (**Figure 3.7**). Interestingly, the stress-strain curve did not show the linear behavior in plastic region in dry conditions. Break strain was not different compared to that of PCL matrixes with and without DS immobilization, suggesting no significant effect of freeze drying process. However, the matrixes with immobilized gelatin failed at much lower tensile strain value when chitosan is added. This could be

due to the reminiscent chitosan on the PCL matrix, although bulk of the material appeared to detach in wet condition. This suggests that the bonding of gelatin to PCL is stronger than that of DS to PCL.

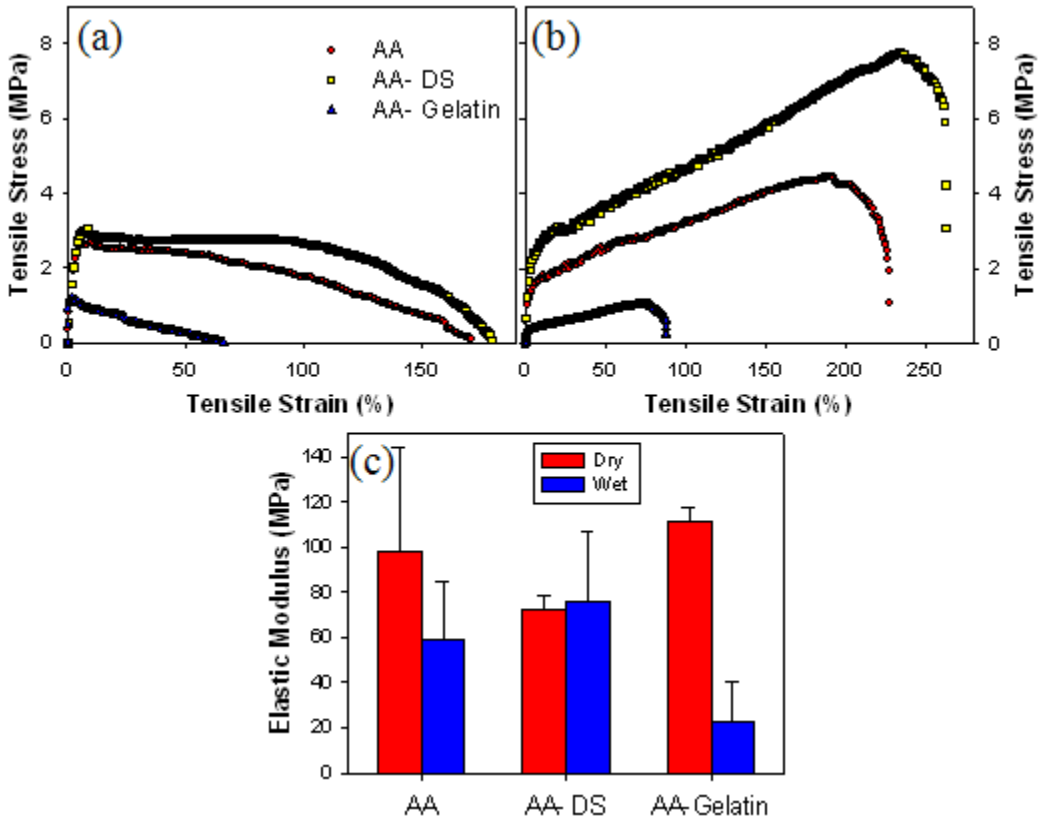

Figure 3.7. Tensile stress-strain plot of PCL matrices with chitosan matrix attached at the bottom side (a) dry condition, (b) wet condition, (c) elastic modulus (E1) of PCL with chitosan matrix formed on the bottom side

From **Figure 3.7b**, we could see that the graph characteristic of the samples after chitosan was added was not different compared to that of the samples without chitosan attachment in wet condition. From The difference in elastic modulus (**Figure 3.7c**) is not significant for dry condition, but, for the test in wet condition, the elastic modulus of all

matrices decrease compare to before chitosan was added, especially for gelatin-immobilized matrices.

Discussion

PCL dissolved in acetic acid spontaneously precipitates into a matrix when in contact with water with increased roughness. Further, the surface charge also is different relative to the matrix formed using chloroform. Using these unique characteristics, previous results showed the possibility of immobilizing gelatin on to PCL, which improved cell adhesion in serum free conditions. Although PCL has been blended with gelatin and other natural polymers, the cost of solvents such as hexafluoro-2-propanol (HFP) [55-57] are relatively expensive compared to acetic acid. Further, they may be toxic to the cells and the body. Thus, the self assembly approach could be utilized to immobilize natural polymers in order to improve its property with simplicity.

This study asked the question whether it is possible to immobilize other molecules and form porous structures. Hence, immobilization of dextran sulfate on to self-assembled PCL matrixes was attempted. Further, effect on tensile properties and viscoelastic properties were tested using 47 kDa PCL. Since the higher the molecular weight has longer degradation time which make it less suitable to be used for tissue regeneration, 47 kDa was selected instead of 80 kDa PCL. The self-assembly did not occur in very low MW (10 kDa and less) PCL.

The tensile test was performed in dry and wet conditions. When samples were tested in dry conditions at room temperature, curves with two distinct slopes were observed in each plot. This behavior changed significantly in wet condition, which may

be due to the hydration and softening due to the nearness to the melting point of PCL affect the structure. Thus the force applied to the sample caused the molecules to reorganize at a specific value of strain and the new structure possesses elastic properties with different elastic modulus. The immobilization of DS and gelatin caused the PCL matrix to become stiffer; there was a significant increase in the first elastic modulus after immobilization but the second elastic modulus did not change. We suspect that the immobilized natural polymer layer in dry condition was broken before the second section of strain and showing no effect was observed for the second elastic modulus. The difference could also be seen in the second elastic modulus of samples in wet condition. The chitosan porous structure was successfully added to the PCL matrix. However, the bonding between the porous structure and PCL matrix was weak and separation was observed upon hydration. This initial attachment could be attributed to the surface roughness of PCL and hydration could differentially expand chitosan and PCL, leading to the separation of phases. One has to attempt forming the porous structure with high MW PCL, as the increased molecular weight increases surface roughness (data not shown). Alternatively, the method of making composites in our previous work [58] could also be used in order to make the chitosan attachment stronger. Performing cell culture to test the cell adhesion improvement for the immobilized matrix is also suggested.

CHAPTER IV

STRESS RELAXATION BEHAVIOR

Realizing the weaknesses of models that are currently used, this study seeks to gain better understanding of stress relaxation behavior of self-assembled PCL, which refers to PCL matrix formed by a unique solvent system (97% acetic acid) to dissolve PCL and form matrices by spontaneous precipitation in water [13], and find an effective mathematical model that can describe this behavior of the material. The first part of this chapter is to study the effect of the strain rate and natural polymers immobilization to PCL stress relaxation behavior. The next part of this work is investigating the potential to model stress relaxation behavior of a pseudo-component model which can describe the stress-strain properties of PCL in multiple strain stages, and provides model interpretability and simplicity. The model was tested with the experimental data using combinations of pseudo-components in order to find the best fit. Self-assembled PCL was chosen for this study due to its hydrophilicity and rough matrix surface. These properties facilitate cell interactions [59, 60], which are the missing properties of traditional chloroform-casted PCL matrix.

Materials and Methods

Sources of Material

Polycaprolactone of 47 kDa (Mn) was purchased from Polysciences (Warrington, PA). Low molecular weight Chitosan (50 kDa based on viscosity), type A porcine skin gelatin (approximately 300 bloom), 500 kDa Dextran Sulfate (contains 0.5-2.0% phosphate buffer salts) and Toluidine Blue O (with 90% dye content, approximately) were obtained from Sigma Aldrich Chemical Co (St. Louis, MO). Glacial acetic acid was purchased from Pharmco Products Inc (Brookfield, CN). Pure ethanol was from AAPER (Shelbyville, KY).

Matrix Generation

First, 3-4 mL of 10% (wt/v) PCL solution prepared in glacial acetic acid was dropped on the surface of water in five-centimeter (two-inch) diameter Teflon dish and air dried until the matrix was completely formed. The matrix was neutralized in ethanol for ten minutes, and then washed with de-ionized water. Since the majority of the published studies use chloroform as a solvent, PCL matrices were also formed by dropping 2 mL PCL solution (10% w/v) in chloroform in the Teflon dish and air drying until the matrix was completely formed.

Effect of Applied Strain Rate to Stress Relaxation Behavior

Stress relaxation tests were performed by an INSTRON 5842 (INSTRON Inc., Canton, MA) mechanical testing machine, as described previously [61]. The self-assembled PCL samples of 12 mm × 30 mm rectangular strips were used, and all the tests

were performed in wet condition (in phosphate-buffered saline (PBS) solution) at 37°C. There were three sets of stress test treatments used for comparing the PCL matrices stress relaxation characteristic and there were five replicates for each experimental treatment:

Treatment i.) constant tensile strain applied at the rate of 3.0% s-1 for 10 seconds, elongating to a 30% strain and then the sample was held at the new length and allowed to relax for 20 seconds. This stage was repeated five times, progressively elongating and holding the sample at 30, 60, 90, 120, and 150% strains.

Treatment ii.) constant tensile strain applied at the rate of 1.0% s-1 for 30 seconds, relax for 30 seconds, then repeat, progressively elongating and holding at 30, 60, 90, 120, and 150% strains.

Treatment iii.) constant tensile strain applied at the rate of 0.6% s-1 for 50 seconds, relax for 100 seconds, then repeat, progressively elongating and holding at 30, 60, 90, 120, and 150% strains.

Each test had five stages of the ramp-and-hold treatment. Three types of graphical representations of the stress response are used for describing stress relaxation behavior. The first graph type shows tensile stress vs. time. The second graph type reveals accumulated stress in each stage. This was created by translating the stress pattern for each stage to the origin. The third graph type shows the relaxation curve, G(t), which plots the relaxation data of the first stage normalized by the highest stress in that stage.

Effect of Natural Polymers Immobilization to Stress Relaxation Behavior

Stress relaxation test was performed by an INSTRON 5842 (INSTRON Inc., Canton, MA) mechanical testing machine, as described previously [61]. The samples of 12 mm x 30 mm rectangular strips were used and all the tests were performed in wet condition at 37°C. The conditions were constant tensile strain applied at the rate of 1.0% s-1 for 30 seconds and then the sample was allowed to relax for 30 seconds. Each test had five stages of the ramp-and-hold treatment. From obtained results, a relaxation curve, G(t), was plotted using the relaxation data of the first stage normalized by the highest stress in that stage.

Model Development

This section was taken from Biomolecular Systems Cluster Proposal "Pseudo-component Viscoelastic Model of Soft Tissues" by R. Russell Rhinehart and Sundar V. Madihally and "Pseudo-component Method for Describing Viscoelastic Properties of PLGA-based Scaffolds" manuscript by R. Russell Rhinehart, Rahul D. Mirani, and Sundar V. Madihally.

Pseudo-component Model Concepts

A material at rest, not stretched, with zero internal stress has original length, height and width of L_0, H_0, and W_0, respectively (**Figure 4.1a**). Viscoelastic components in the material, which are represented as line segments in **Figure 4.1**, are oriented randomly at this state. The term "component" represents a general class of functional relationships such as folded sections in macromolecule, which could be unfolded in response to strain. When external loading is applied, the component will

stretch, and internal stress will be developed. The new material length is now L = $L_0(1+\varepsilon)$ and if material volume remains constant, the lateral contraction creates new height and width of H and W, respectively (**Figure 4.1b**). The elongated material is held for a period of time while the stress is partially relaxed (**Figure 4.1c**) by redistribution of the internal structure. Then if strain were removed, the material would shrink to a length at which internal stress was all relieved (**Figure 4.1d**) and the internal structure is equivalent to the initial at-rest structure in **Figure 4.1a**. The length in **Figure 4.1d** is called L_{equ} and the stress in **Figure 4.1c** is that which would have happen if **Figure 4.1d** had been stretched with a strain of $\varepsilon = L(1+\varepsilon)/L_{equ}$

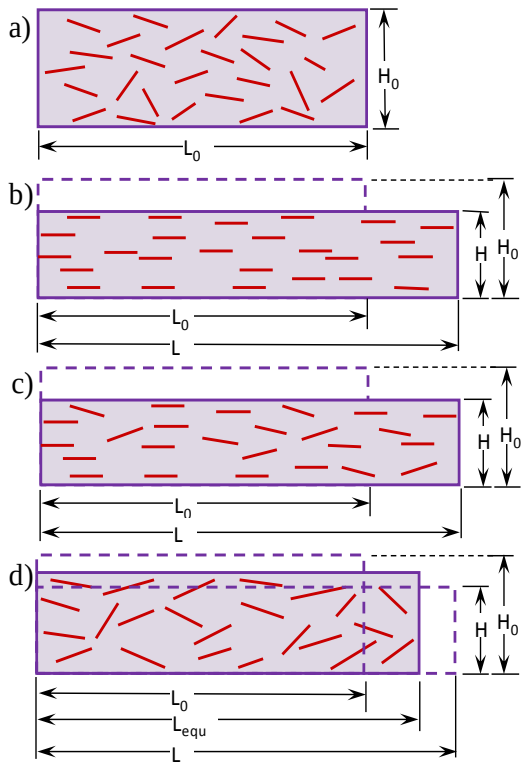

Figure 4.1. Concept of viscoelastic stress relaxation (a) material at rest (b) material elongated and stressed (c) material elongated and held while stress partially relaxes and (d) material released

Four pseudo-components are proposed to explain the relaxation behavior of the material.

Pseudo-Component Concept 1: Hyperelastic spring – This concept describes a material which does not relax internal stress. The material would snap back to its original size and structure if external load was removed. A hyperelastic spring has nonlinear stress response to strain as illustrated by either **Figure 4.2a** or curve i) in **Figure 4.2b**.

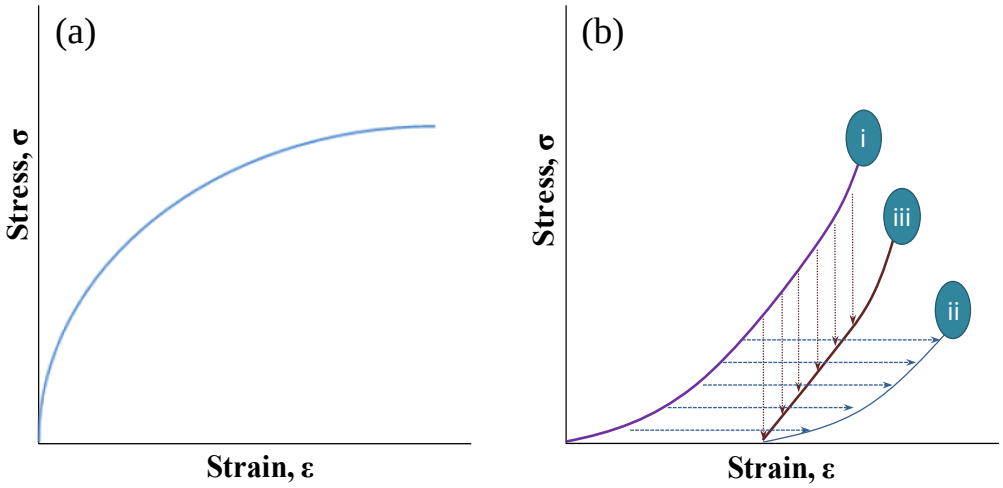

Figure 4.2. Conceptual illustration of (a) Instantaneous stress-strain relation and (b) the difference in material response after relaxation i) hyperelastic spring, ii) reform, and iii)

Pseudo-Component Concept 2: Spring-and-dashpot – This concept does not consider any change in material H and W dimensions when elongation occurs. Spring-and-dashpot components will relax to the original zero stress state when held elongated at any length $L = L_0(1+\varepsilon)$.

Pseudo-Component Concept 3: Reform – This concept includes the necking-in cross-sectional area reduction due to material stretching from length L_0 to length L. Additionally, while holding the elongated material at length, L, the components in the

material will partially reform to their original random orientation as illustrated in **Figure 4.1c**. If the loading is removed prior to total relaxation, the material will recover to a permanently elongated state of length, L_{equ} ($L > L_{equ} > L_0$) (**Figure 4.1d**) with smaller cross-section area, but with the original random, stress-free component structure. Alternatively, if the strain is not relieved when partial relaxation has occurred, the stress will equal to the stress of the material with original length, L_{equ} which was stretched to length L. The effective strain would be equal to $(L-L_{equ})/L_{equ}$. The curve segment (ii) in **Figure 4.2b** illustrates the behavior of the stress after the material is relaxed according to this concept.

Pseudo-Component Concept 4: Retain – This concept also accounts for cross-sectional area reduction when the material is stretched. However, while holding the elongated material at length, L, the components in the material will retain the stretched orientation and relieve the stress by setting to the new structure orientation. If the strain is continued after the relaxation has already occurred, the curve pattern of the stress will continue from the pre-oriented molesules at the holding strain position. The curve segment (iii) in **Figure 4.2b** illustrates the behavior of the stress after the material is relaxed according to this concept.

Mathematical Statement

The pseudo-component model used in this study attributes the overall viscoelastic response to several parallel pseudo-components, sharing the same external deformation, additively combining stress forces, and relaxing at individual rates. The use of a numerical method to solve the model eliminates the linearization and truncation

assumptions of an analytical model. **Figures 4.2a** and **4.2b (i)** illustrate nonlinear instantaneous stress-strain relations for a pseudo-component, commonly labeled "hyperelastic", and modeled as

$$\sigma_i = A_i(e^{B_i\varepsilon_i} - 1) \tag{1}$$

where the subscript "i" indicates the i^{th} pseudo-component. Coefficients A and B must have the same sign. **Figure 4.2a** results for A, B > 0 and **Figure 4.2b** for A, B < 0.

Also, in this work, each pseudo-component which undergoes internal material deformation is modeled as having a first-order rate of internal stress relaxation, toward complete relaxation of zero stress at infinite time. With no strain-rate-induced stress, the relaxation model is:

$$\tau_i \frac{d\sigma_i}{dt} + \sigma_i = 0,\ \sigma_i(t=0) = \sigma_0 \tag{2}$$

For the material internal deformation concept of **Figure 4.1**, if the strain is instantaneously applied at one stage, then Equation (1) models the stress, and if the elongation is then held for a period of time, Equation (2) reveals the stress relaxation. However, if the material is strained at a particular rate while it is relaxing, then rigorous derivation reveals that Equation (2) needs to include the rate that internal stress is "injected" due to the rate of external strain.

$$\tau_i \frac{d\sigma_i}{dt} + \sigma_i = \tau_i \frac{\partial\hat{\sigma}_i}{\partial\varepsilon}\frac{d\varepsilon_i}{dt} = \tau_i A_i B_i \exp(B_i \frac{Lequ_i}{L}\varepsilon)\frac{Lequ_i}{L}\frac{d\varepsilon}{dt},\ \sigma_i(t=0) = \sigma_0 \tag{3a}$$

$$\tau_i \frac{d\sigma_i}{dt} + \sigma_i = \tau_i \frac{\partial\hat{\sigma}_i}{\partial\varepsilon}\frac{d\varepsilon_i}{dt} = \tau_i A_i B_i \exp(B_i\varepsilon)\frac{d\varepsilon}{dt},\ \sigma_i(t=0) = \sigma_0 \tag{3b}$$

Equations (3a) and (3b) represent the internal viscous deformation mechanism illustrated in **Figure 4.1**, with the nonlinear "AB" instantaneous stress-strain constitutive

model of Equation (1). Equation (3a) is for the reform internal structure recovery in time (**Figure 4.2b** curve ii) and is similar to a nonlinear spring-and-dashpot model. Equation (3b) is for the structure-setting retain mechanism of stress relief (**Figure 4.2b** curve iii); it is not equivalent to the spring-and-dashpot model, because the "spring" is not permitted to return to its zero elongation state.

Equations (3a) and (3b) can be solved by any of many numerical methods, and can be used for either strain- or stress-induced deformation, free relaxation after deformation, and either tensile or compressive influences. The use of numerical methods for solution permits any stress or strain history to be modeled.

Given the partially relaxed stress of pseudo-component "i" from Equation (3a), at the end of time increment Δt, the equivalent strain on the film component can be calculated by the inverse of Equation (1)

$$\varepsilon_i(t+\Delta t) = \ln\left(\frac{\sigma_i(t+\Delta t)}{A_i} + 1\right) / B_i \qquad (5)$$

The value of the strain from Equation (5) would be the equivalent strain, from which the equivalent length of pseudo-component "i" would be calculated by

$$Le_i(t+\Delta t) = L_0\ \ 1+\varepsilon_i(t+\Delta t) \qquad (6)$$

Which would end the analysis of viscoelastic processes within time period, Δt. At the updated time, t, initiating the next change in ε, $Le_i(t)$ is that calculated from Equation (6). When the external strain (the apparent strain, ε_0) instantly changes, the length of the film is

$$L(t) = L_0\ \ 1+\varepsilon_0(t) \qquad (7)$$

The new effective strain on the pseudo-component is

$$\varepsilon_i(t) = \frac{L(t) - Le_i(t)}{Le_i(t)} \tag{8}$$

The initial value for Le_i is L_0. Sequential applications of Equations (7), (8), (3a) or (3b), (5), and then (6) model stress vs. time for each internal deforming pseudo-component. As with any numerical method, the time interval Δt needs to be appropriately small (depending on the numerical algorithm) relative to time-constants and to time periods for changes in the strain rate.

Composite Models

Mathematical models of the materials are created by adding the stress from sets of pseudo-component equations. Each of the composite models has a structure which places pseudo-components in parallel, as illustrated in **Figure 4.3**. Part of the composite model description is the number of parallel elements, and the other part is the pseudo-component type for each element. This work will use the term architecture to describe the structure and element types in the composite model.

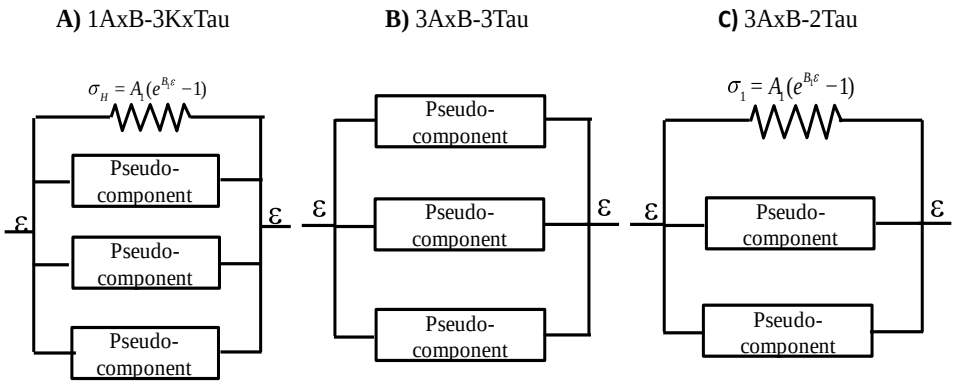

Figure 4.3. Model conceptual illustration (A) 1AxB-3KxTau (B) 3AxB-3Tau and (C) 3AxB-2Tau

Initial screening investigation explored three architectures:

Architecture A) 1AxB-3KxTau (8 parameters) – 4 elements in parallel. One is a nonlinear spring and three are linear spring ($\sigma = k\varepsilon$) and dashpot components.

Architecture B) 3AxB-3Tau (9 parameters) – 3 elements in parallel. Each is nonlinear viscoelastic "retain" element of Equation (3b).

Architecture C) 3AxB-2Tau (8 parameters) – 3 elements in parallel. One is a nonlinear spring and two are nonlinear viscoelastic "retain" elements of Equation (3b).

The best model selection is based on two criteria a) the value of the sum of squared errors (SSD), and b) model complexity. Screening revealed that Architecture C was the best model. Even with 4 components, the linear "springs" of Architecture A did not capture the stress response as well as Architecture B. Regression assigned to one of the pseudo-components in Architecture B gave an exceedingly large value for τ, meaning that one of the components relaxed at a very low rate, effectively making it a hyperelastic spring, which suggested Architecture C, which modeled the σ response as well as Architecture B but with one fewer parameter.

Then that structure with different combinations of pseudo-components was tested. Accordingly, the combinations of pseudo-components were:

Combination 1 – one hyperelastic and two spring-and-dashpot pseudo-components.

Combination 2 - one hyperelastic and two reform pseudo-components.

Combination 3 - one hyperelastic and two retain pseudo-components.

Combination 4 – one each hyperelastic, spring-and-dashpot, and retain pseudo-component.

Combination 5 - one each hyperelastic, spring-and-dashpot, and reform pseudo-component.

Combination 6 - one each hyperelastic, retain, and reform pseudo-component.

Model parameters were obtained by nonlinear regression from random initial values with 25 independent optimization initializations. After selecting the best-of-25, 1,000 additional optimization iterations were performed to confirm the model parameter values.

Results

Effect of Applied Strain Rate to Stress Relaxation Behavior

Three sets of testing conditions were performed on PCL matrices in order to study the effects of loading rates and relaxation time on stress relaxation behavior of PCL as illustrated in **Figures 4.4a**, **4.4b**, and **4.4c**. The behaviors of PCL matrices in all three conditions were similar. The first stage showed the highest stress accumulation, and there was little difference in stress accumulation of successive stages (**Figure 4.4d-4.4f**). This behavior is consistent with previous studies [13]. The stress accumulation at 0.6% s^{-1} loading rate was the highest of the three testing conditions (**Figure 4.4d**), but similar to that from loading rates of 1.0% s^{-1} and 3.0% s^{-1} (**Figure 4.4e and 4.4f**).

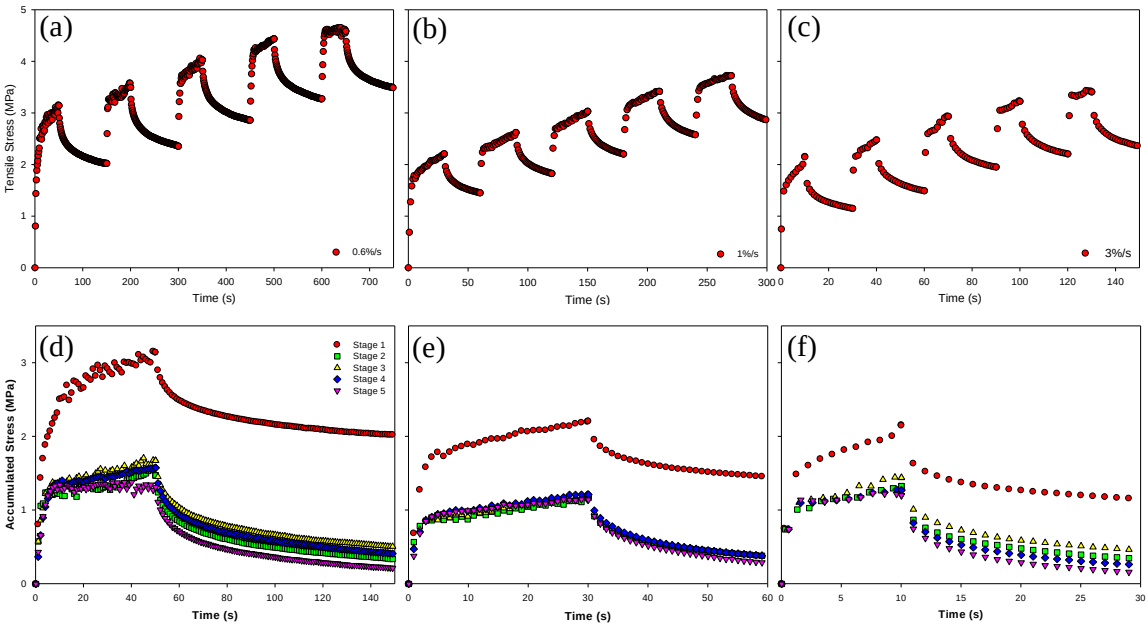

Figure 4.4. Stress relaxation plot at different loading rate (a) 0.6%/s loading for 50 s and 100 s relaxation time (b) 1.0%/s loading for 30 s and 30 s relaxation time and (c) 3.0%/s loading for 10 s and 20 s relaxation time (d) stress accumulation of 0.6%/s strain rate (e) stress accumulation of 1.0%/s strain rate (f) stress accumulation of 3.0%/s strain rate

Also, the average relaxation curve, G(t) (**Figure 4.5**), reveals relaxation patterns of the three testing conditions were not statistically different. The error bars indicate the 95% confidence interval on the average of 5 test replicates. These results indicate that the effect of the strain rate is insignificant on relax rates and on subsequent strains. However, strain rate does have a substantial impact on the σ from the first stage.

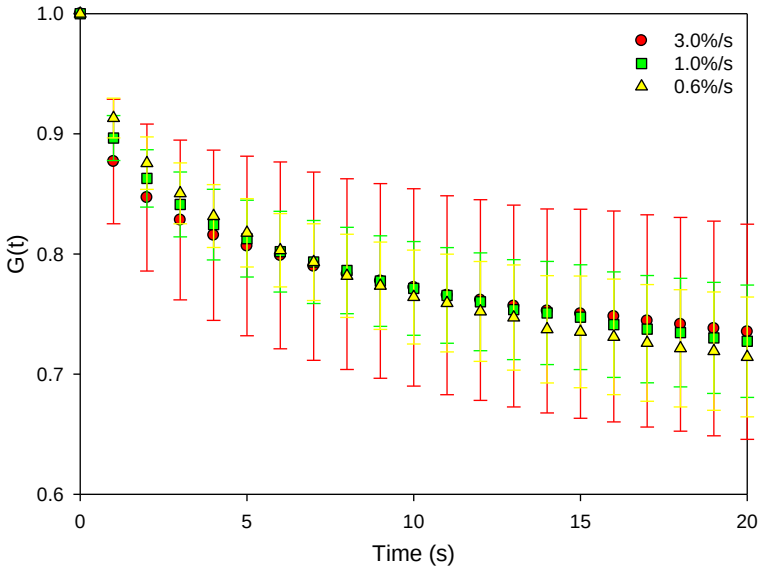

Figure 4.5. Relaxation function, G(t), plot from the characteristic trend of the first stage of each strain rate with the error bars represented the standard deviations from 5 tests.

Effect of Natural Polymers Immobilization to Stress Relaxation Behavior

There was no statistically significant difference in the stress relaxation test for both PCL with and without immobilized natural polymers (**Figure 4.6**). Chloroform-casted PCL matrices had higher stress accumulation than self assembled PCL matrices. In the first stage, all samples showed the highest stress values and there was no difference in other stages. Compared to our previous study in the same condition [13], the stress relaxation trend and the value of stress accumulation were similar for both chloroform-casted and self assembled PCL matrices in despite of the difference in molecular weight.

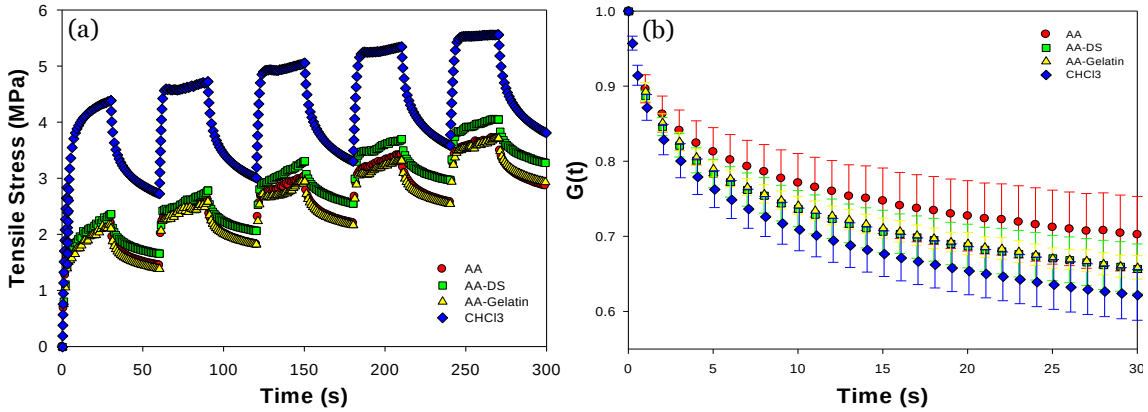

Figure 4.6. Stress relaxation of PCL matrices (a) Effect of multiple ramp-hold stages, (b) Relaxation function, G(t), of PCL matrices.

The plot of relaxation function, G(t) (**Figure 4.6b**), of all PCL matrices showed about 20%-30% stress relaxation capability after the stress was applied in the first stage.

Selection of the Most Appropriate Model

Since the strain rate did not affect much on the stress relaxation behavior, the selection of testing conditions for initial architecture screening was the intermediate 1%/s strain rate. Three architectures (A, B, C) were fitted to the stress relaxation experimental data of self-assembled and chloroform-casted PCL matrices. **Figure 4.7** illustrates the characteristic data set from the 5 replicate tests.

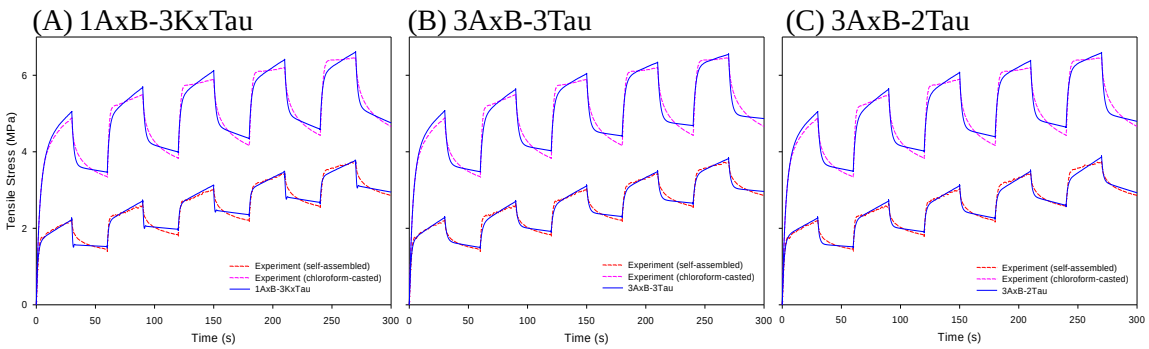

Figure 4.7. Comparison of each model fitting with the experimental data at 1% s^{-1} strain rate (A) 1AxB-3KxTau (B) 3AxB-3Tau and (C) 3AxB-2Tau

For self-assembled PCL, the average SSD of Architecture A, B, and C were 2.4, 1.4, and 1.5, respectively (Tables 4.1, and 4.2, and Combination 3 from Table 4.3). Architecture A obviously failed in fitting the relaxation phase (**Figure 4.7A**) and had the worst SSD for self-assembled PCL. Although both Architecture B and C had similar SSD values, Architecture C was chosen over Architecture B for several reasons. It has fewer parameters (less complex). Further, one τ value in Architecture B was always exceedingly large, suggesting that one pseudo-component does not relax, reducing it to a nonlinear spring, which is the basis for Architecture C. Analysis of the data for the chloroform-casted films leads to the same conclusions since Architecture C gave the lowest SSD (**Table 4.1**, **4.2**, and **4.3** – Combination 3).

Table 4.1 Average parameter values with standard deviations of 1AxB-3KxTau (Architecture A) with one hyperelastic and three linear spring-and-dashpot pseudo-components

Parameters (units)	$CHCl_3$	AA
Ax1 (MPa)	-1.91 ± 0.88	-0.99 ± 0.19
B1 (dimensionless)	-26.46 ± 5.37	-56.81 ± 6.37
Kx2 (MPa)	40.45 ± 66.70	2061 ± 1933
Tau2 (s)	1.51 ± 0.19	0.0021 ± 0.0014
Kx3 (MPa)	52.85 ± 42.97	20245 ± 5261
Tau3 (s)	26.16 ± 42.70	0.0027 ± 0.0003
Kx4 (MPa)	2.73 ± 1.21	1.89 ± 0.39
Tau4 (s)	259 ± 178	449 ± 212
SSD (MPa^2)	**11.04 ± 2.37**	**2.38 ± 0.40**

Table 4.2 Average parameter values with standard deviations of 3AxB-3Tau (Architecture B) with three retain pseudo-components

Parameters (units)	$CHCl_3$	AA
Ax1 (MPa)	736 ± 170	377 ± 216
B1 (dimensionless)	0.11 ± 0.02	0.12 ± 0.07
Tau1 (s)	1.76 ± 0.21	1.63 ± 0.06
Ax2 (MPa)	-2.52 ± 0.26	-1.09 ± 0.18
B2 (dimensionless)	-27.41 ± 9.53	-77.15 ± 11.18
Tau2 (s)	423 ± 149	329 ± 380
Ax3 (MPa)	-9.12 ± 2.46	-5.41 ± 1.14
B3 (dimensionless)	-0.43 ± 0.14	-0.49 ± 0.09
Tau3 (s)	748 ± 34	$2.04x10^{14} \pm 2.62x10^{14}$
SSD (MPa^2)	**12.38 ± 2.65**	**1.37 ± 0.15**

Table 4.3 Average parameter values with standard deviations of 3AxB-2Tau (Architecture C) with different pseudo-component combinations: Combination 1 – one hyperelastic and two spring-and-dashpot pseudo-components, Combination 2 - one hyperelastic and two reform pseudo-components, Combination 3 - one hyperelastic and two retain pseudo-components, Combination 4 – one each hyperelastic, spring-and-dashpot, and retain pseudo-component, Combination 5 - one each hyperelastic, spring-and-dashpot, and reform pseudo-component, and Combination 6 - one each hyperelastic, retain and reform pseudo-component

a) PCL-$CHCl_3$

Parameters	Combination 1	Combination 2	Combination 3	Combination 4	Combination 5	Combination 6
Ax1 (MPa)	-3.19 ± 0.49	-2.70 ± 0.52	-2.47 ± 0.41	21.11 ± 3.72	-2.51 ± 0.37	-4.01 ± 0.60
B1 (dimensionless)	-0.92 ± 0.57	-6.36 ± 1.10	-29.10 ± 8.50	0.08 ± 0.02	-17.86 ± 2.76	-3.34 ± 0.80
Ax2 (MPa)	-6.47 ± 1.21	-3.20 ± 0.40	848 ± 357	15.22 ± 9.80	-2.30 ± 0.28	2.76 ± 1.04
B2 (dimensionless)	-16.77 ± 5.56	-87.88 ± 20.44	0.12 ± 0.06	9.28 ± 8.03	-57.67 ± 10.43	1.81 ± 0.09
Tau2 (s)	1.33 ± 0.19	4.97 ± 0.15	1.54 ± 0.07	1.55 ± 0.12	4.70 ± 0.49	2.21 ± 1.05
Ax3 (MPa)	-2.86 ± 0.29	0.55 ± 0.13	9.59 ± 5.33	-2.80 ± 0.47	1.66 ± 0.52	-3.26 ± 0.83
B3 (dimensionless)	-28.58 ± 9.78	2.29 ± 0.30	0.30 ± 0.07	-18.60 ± 6.21	0.80 ± 0.14	-68.21 ± 23.21
Tau3 (s)	100 ± 30	158 ± 20	124 ± 21	917 ± 209	498 ± 244	8.22 ± 4.75
SSD (MPa^2)	**6.60 ± 2.23**	**28.94 ± 7.42**	**10.74 ± 2.51**	**16.08 ± 5.42**	**6.42 ± 2.38**	**16.59 ± 2.76**

b) PCL-AA

Parameters	Combination 1	Combination 2	Combination 3	Combination 4	Combination 5	Combination 6
Ax1 (MPa)	-5.45 ± 2.49	-0.88 ± 0.17	-0.99 ± 0.20	-5.92 ± 2.26	-4.61 ± 1.03	-4.30 ± 0.94
B1 (dimensionless)	-0.45 ± 0.40	-13.19 ± 5.13	-65.42 ± 13.51	-0.50 ± 0.31	-0.64 ± 0.36	-0.68 ± 0.36
Ax2 (MPa)	-1.08 ± 0.14	-1.21 ± 0.14	-388 ± 76	-0.89 ± 0.12	6.48 ± 0.18	38.41 ± 15.72
B2 (dimensionless)	-41.30 ± 6.02	-292 ± 92	-0.12 ± 0.07	-76.83 ± 14.90	5.20 ± 0.55	0.53 ± 0.11
Tau2 (s)	1.78 ± 0.11	4.00 ± 0.66	1.49 ± 0.24	4.01 ± 0.23	1.34 ± 0.10	1.36 ± 0.12
Ax3 (MPa)	-1.20 ± 0.16	2.06 ± 0.54	10.22 ± 4.25	-0.97 ± 0.16	-1.18 ± 0.14	-1.38 ± 0.14
B3 (dimensionless)	-68.72 ± 5.17	0.81 ± 0.09	0.19 ± 0.06	-59.63 ± 6.53	-87.46 ± 13.14	-96.38 ± 11.50
Tau3 (s)	99.27 ± 18.94	384 ± 91	327 ± 140	270 ± 90	74.24 ± 8.81	56.14 ± 10.33
SSD (MPa^2)	**0.44 ± 0.11**	**2.78 ± 0.58**	**1.52 ± 0.30**	**0.72 ± 0.20**	**1.11 ± 0.15**	**0.81 ± 0.10**

Then, different combinations of pseudo-components were tested with the chosen model architecture. See **Figure 4.8** for characteristic trends. Combination 1 has significantly the lowest SSD for self-assembled PCL. For chloroform-casted PCL, there is insignificant difference between Combinations 5 and 1. Therefore, Combination 1 was chosen as the best fit with both data. However, the spring-and-dashpot model does not account for a change in sample cross-sectional area. Combination 2 (SSD = 2.8 MPa^2 for self-assembled and SSD = 28.9 MPa^2 for chloroform-casted) failed to follow the trend of the experimental data (**Figure 4.8b**), as evidenced by the sequential decrease in model-predicted trend relative to the experimental data for both self-assembled and chloroform-casted PCL. Combination 3 (SSD = 1.5 MPa^2 for self-assembled and SSD = 10.7 MPa^2 for chloroform-casted) showed that both the stress accumulation and the stress relaxation would be increased in each stage for both self-assembled and chloroform-casted PCL (**Figure 4.8c**).

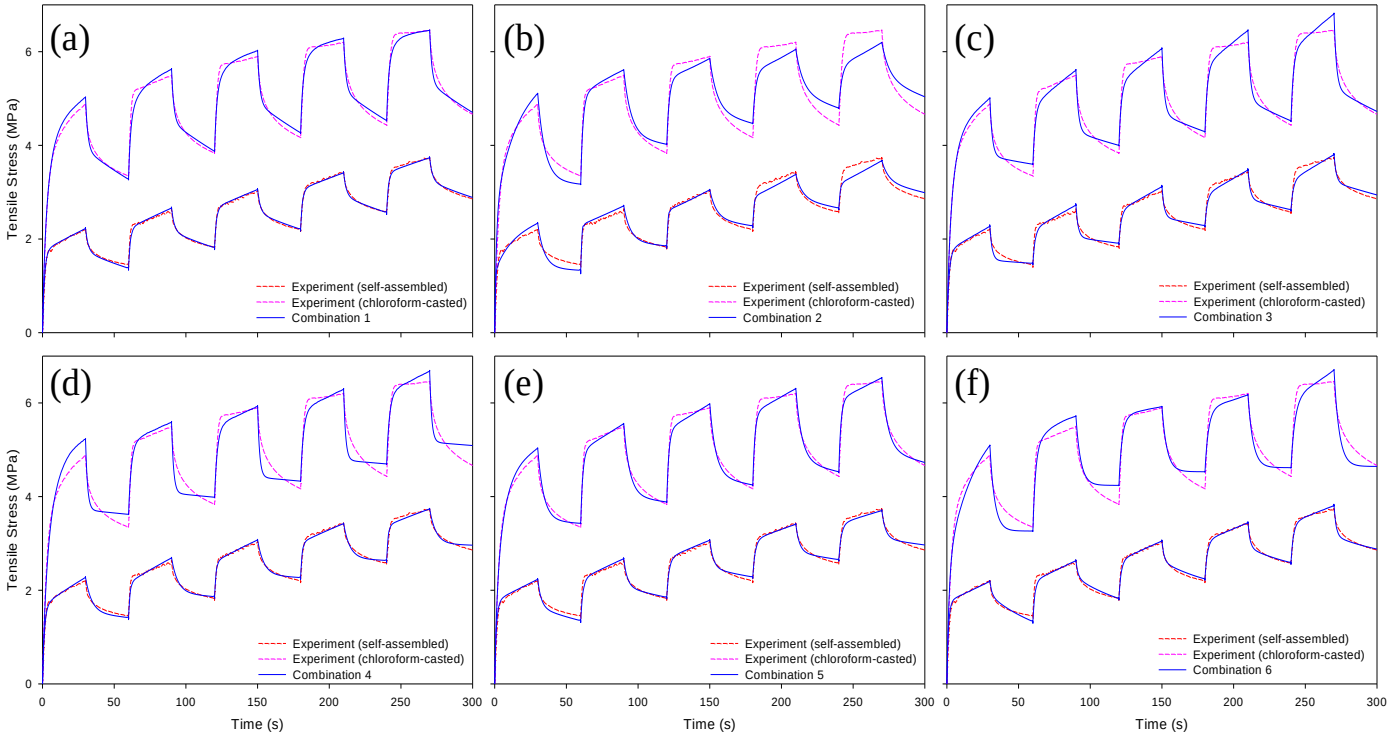

Figure 4.8. Comparison of Architecture C with each characteristic trial pseudo-component combination at 1% s^{-1} strain rate (a) Combination 1 – one hyperelastic and two spring-and-dashpot pseudo-components (b) Combination 2 - one hyperelastic and two reform pseudo-components (c) Combination 3 - one hyperelastic and two retain pseudo-components (d) Combination 4 – one each hyperelastic, spring-and-dashpot, and retain pseudo-component (e) Combination 5 - one each hyperelastic, spring-and-dashpot, and reform pseudo-component (f) Combination 6 - one each hyperelastic, retain and reform pseudo-component

However, when different pseudo-components were combined, differences between self-assembled and chloroform-casted PCL were observed. For self-assembled PCL, Combination 4 - combination of dashpot with retain (SSD = 0.7 MPa^2) and Combination 5 - combination of dashpot with reform (SSD = 1.1 MPa^2) showed some improvement from Combination 3 and 2 respectively. The results were different for chloroform-casted PCL. Combination 4 (SSD = 16.1 MPa^2) was worse than Combination 5 (SSD = 6.4 MPa^2), which was equivalent to Combination 1 (SSD = 6.6 MPa^2). While the experimental data showed gradual relaxation, Combination 4 model would rapidly relax and then almost not relax at all (**Figure 4.8d**). Since a spring-and-dashpot pseudo-component was used in these combinations, the aim of finding a more realistic explanation to the stress relaxation mechanism was not completely accomplished. For this reason, Combination 6, which does not have spring-and-dashpot pseudo-component in the composite model, was tested. This composite model gave the SSD value of 0.8 MPa^2 for self-assembled PCL. It could fit well with the experimental data of the self-assembled PCL and also provide more realistic explanation for the mechanism than the spring-and-dashpot pseudo-component. On the contrary, this pseudo-component combination could not improve the fitting of the model to the chloroform-casted PCL data. It could not maintain similar graph pattern in each cycle and the SSD value (SSD = 16.6 MPa^2) was higher than that of the dashpot-only pseudo-component.

Discussion

This study focused on stress relaxation behavior of the self-assembled PCL matrix, at conditions designed to imitate the in vivo environment. Results showed that, at low strain rate (0.1-3% s-1), there was little effect of the strain rate to stress relaxation behavior of PCL matrix, which is similar to findings in a previous study [13] at different strain rate conditions and PCL molecular weight.

However, this stress relaxation behavior of PCL matrices was different from 50:50 poly-lactide-co-glycolide (PLGA) samples and also from small intestinal submucosa (SIS) [62]. Although the stress accumulation of PLGA matrix was decreased in successive stages, the stress accumulation of SIS was increased in successive stages. However, the stress accumulation of all PCL samples showed the highest stress value only in the first stage and there was no difference in other stages. This highest stress value in the first stage could be viewed as "preconditioning" of PCL matrix, which was in contrast of PLGA and SIS that the applied strain would affect the stress relaxation property of PLGA and SIS in every stage.

From the results of the stress relaxation test on immobilized PCL, there was no difference between the matrices with and without the immobilized natural polymers, probably the natural polymers could break before the second section of strain. Also, molecular weight of PCL had no effect on the relaxation characteristic, as the observed relaxation properties with 47 kDa were similar to previous published reports using 80 kDa samples. All samples showed the highest stress values in the first stage and there was no difference in other stages. The observed behavior was different from other reports on electrospun PCL fibers [10]. These differences could be attributed to the

differences in loading rate and relaxation time, the wet and dry environment and the temperature as the processing.

In order to explain stress relaxation behavior in multiple stages, three model architectures were tested, and Architecture C chosen as best fit to experimental data for both chloroform-casted and self-assembled PCL matrices. Within Architecture C, pseudo-component Combination 1, which contains one hyperelastic spring and two spring-and-dashpot pseudo-components, provided the best fit (lowest SSD), in spite of the spring-and-dashpot concept not accounting for material cross-sectional area reduction. The reform and retain models are based on a uniform cross-sectional area reduction upon length elongation. Observation of experimental samples, however, reveals some width reduction in the center, not the clamped ends, and internal tearings. Although the retain pseudo-components provided a best fit elsewhere [61], the behavior of PCL matrices was slightly more consistent with the uniform cross sectional area of the spring-and-dashpot concept.

CHAPTER V

CONCLUSIONS AND RECOMMENDATIONS

Conclusions

This study focused on the potential of self-assembled PCL matrices as scaffolds for tissue regeneration. The possibility of natural polymers immobilization, which may help improving cell regulation on PCL matrices, as well as its effect on self-assembled PCL matrices mechanical properties were investigated. This study also explored the stress relaxation behavior of the matrices to gain better understanding of PCL matrices formed by this novel method. According to the specific aims, two conclusions can be summarized for this study.

SPECIFIC AIM 1: Immobilization of Natural Polymers

a) Self-assembled PCL matrices have the sidedness property due to the different surface in contact when the matrix was formed. During the matrix formation, the top side is in contact with air, but the bottom side is in contact with water and different surface architecture is created.

b) Immobilization of dextran sulfate and gelatin onto self-assembled PCL is possible. The immobilized natural polymers do not have much effect on the surface architecture and tensile properties since the difference is statistically insignificant.

c) Chitosan porous structure attachment to self-assembled PCL is very weak and the bond can easily be destroyed by hydration. Consequently, the chitosan-incorporated PCL matrix cannot be used as scaffolds since they are going to be used as synthetic tissues in human body, which is hydrated environment.

SPECIFIC AIM 2: Analysis of Stress Relaxation Behavior

a) The effect of strain rate on the stress relaxation behavior of self-assembled PCL matrix was statistically insignificant at these experimental conditions. The stress accumulation was the highest in the first stage, but became similar in the successive stages, which could be viewed as the behavior after the "molecular orientation preconditioning".

b) The natural polymers immobilization has little effect on the stress relaxation behavior of self-assembled PCL matrix. The stress accumulation pattern in each stage was similar to what is described in the previous conclusion, probably due to the breaking of the natural polymers before the second stage of the loading phase.

c) In order to understand the stress relaxation behavior better, a pseudo-component model was developed and fit with the experimental data. The combination of hyperelastic spring and spring-and-dashpot elements provided the best fit with this data. Although reform and retain pseudo-component concepts did not

provide the best fit, all forms of the pseudo-component model showed good fits in multiple stages. This is an improvement over traditional QLV model ability, and shows promise for being the modeling approach suitable for describing viscoelastic behavior of biomaterials.

d) With 8 parameters, the pseudo-component modeling approach can accept any strain history, including sequential strain-and-hold stage, and provide good fits to experimental data. Moreover, the pseudo-components have a direct relation of molecular structure to physical meaning. By contrast, although the modified QLV model with 5 parameters can describe a sequence of stages [63], it is still unable to explain the stress relaxation behavior of materials.

Recommendations

1. Since the self-assembly technique for forming PCL matrices has been recently developed, there are many aspects about this method that could be explored such as the effect of water-bath temperature, vibration, or pH of water-bath to the formed matrices surface architecture and properties. We could gain better understandings about the self-assembled PCL by studying about these aspects.
2. Since the natural polymers immobilization to PCL matrix is possible, the stability of the attachment should be tested. Due to the fact that chitosan porous structure attachment is weak, the immobilized DS and gelatin need to be confirmed that the immobilization is strong enough to be used in hydrated condition.
3. Evaluation of cellular activity on immobilized PCL matrices is suggested for testing the improvement of cell adhesion in comparison with plain self-assembled

matrices. PCL matrices have poor bioregulatory activity, which is its major disadvantage. The immobilization of natural polymers may help improving the limited cell regulation of PCL matrices, which will benefit in its use as scaffolds to make synthetic tissue for tissue regeneration.

4. The pseudo-component model shows its potential for describing stress relaxation behavior of material in sequential stages. However, the uniform cross-sectional area reduction is not true for PCL matrices and this may be the cause of the deviation from experimental data. If the stable necking is taking into account of the model concept, there may be some improvement to the fitting.
5. Although the pseudo-component model is derived based on explainable physical phenomena, the meaning of each parameter cannot be clearly seen with just one material. The model should be used with other biomaterials, which can be naturally or synthetically formed matrices, either from natural or synthetic polymers that have different mechanical properties, in order to explain what each parameter is represented. Combining the tensile properties with the relaxation behavior, the meaning of the parameter values can be interpreted by comparing the values with those of other biomaterials.
6. The parameters obtained are the average values of the optimized parameters from each experimental data. These parameters are the average from all sets of parameters that represent the characteristic of each sample and may not be the most appropriate parameters to be used as the representation of self-assembled PCL matrix. The average values of parameters may not give the average characteristic of self-assembled PCL stress relaxation when they are used in the

model. Parameters of the average stress relaxation data from the experiment should be found and compared. For reliable results, at least ten sets of stress relaxation data should be used for finding the average values of stress as a function of time. Then, these data will be used for finding the model parameters, which will be the parameters represent the characteristic of self-assembled PCL.

REFERENCES

1. Langer, R. and J.P. Vacanti, *Tissue engineering.* Science, 1993. **260**(5110): p. 920-6.
2. Woodruff, M.F., *Transplantation of the Kidney in Man.* Triangle, 1964. **19**: p. 208-16.
3. Wright, W.K., *Plastic and reconstructive surgery 1966.* Arch Otolaryngol, 1968. **88**(5): p. 556-63.
4. Kolff, W., et al., *The artificial kidney: a dialyser with a great area. 1944 [classical article].* J Am Soc Nephrol, 1997. **8**(12): p. 1959-1965.
5. Yuen, J.C., et al., *Long-term sequelae following median sternotomy wound infection and flap reconstruction.* Ann Plast Surg, 1995. **35**(6): p. 585-9.
6. Raghavan, D., et al., *Physical characteristics of small intestinal submucosa scaffolds are location-dependent.* J Biomed Mater Res A, 2005. **73**(1): p. 90-6.
7. Zielinski, B.A. and P. Aebischer, *Chitosan as a matrix for mammalian cell encapsulation.* Biomaterials, 1994. **15**(13): p. 1049-56.
8. Cheng, M., et al., *Study on physical properties and nerve cell affinity of composite films from chitosan and gelatin solutions.* Biomaterials, 2003. **24**(17): p. 2871-80.
9. Kang, H.W., Y. Tabata, and Y. Ikada, *Fabrication of porous gelatin scaffolds for tissue engineering.* Biomaterials, 1999. **20**(14): p. 1339-44.
10. Duling, R.R., et al., *Mechanical characterization of electrospun polycaprolactone (PCL): a potential scaffold for tissue engineering.* J Biomech Eng, 2008. **130**(1): p. 011006.
11. Sarasam, A. and S.V. Madihally, *Characterization of chitosan-polycaprolactone blends for tissue engineering applications.* Biomaterials, 2005. **26**(27): p. 5500-8.
12. Lin, H.B., et al., *Synthesis, surface, and cell-adhesion properties of polyurethanes containing covalently grafted RGD-peptides.* J Biomed Mater Res, 1994. **28**(3): p. 329-42.
13. Pok, S.W., K.N. Wallace, and S.V. Madihally, *In vitro characterization of polycaprolactone matrices generated in aqueous media.* Acta Biomater. **6**(3): p. 1061-8.
14. Nerem, R.M. and A. Sambanis, *Tissue engineering: from biology to biological substitutes.* Tissue Eng, 1995. **1**(1): p. 3-13.
15. Langer, R., et al., *Tissue Engineering: Biomedical Applications.* Tissue Engineering, 2007. **1**(2): p. 151-161.
16. Rose PJ, M.H., Bikales NM, Overberger CG, Menges G, Kroschwitz JI, editors, *Encyclopedia of polymer science and engineering*. second ed. Vol. 7. 1989, New York, USA: Wiley.
17. Dubruel, P., et al., *Porous gelatin hydrogels: 2. In vitro cell interaction study.* Biomacromolecules, 2007. **8**(2): p. 338-44.
18. Yin, Y., et al., *Preparation and characterization of macroporous chitosan-gelatin/beta-tricalcium phosphate composite scaffolds for bone tissue engineering.* J Biomed Mater Res A, 2003. **67**(3): p. 844-55.
19. Mao, J., et al., *Study of novel chitosan-gelatin artificial skin in vitro.* J Biomed Mater Res A, 2003. **64**(2): p. 301-8.
20. Khor, E. and L.Y. Lim, *Implantable applications of chitin and chitosan.*

Biomaterials, 2003. **24**(13): p. 2339-49.
21. Hu, S.G., C.H. Jou, and M.C. Yang, *Protein adsorption, fibroblast activity and antibacterial properties of poly(3-hydroxybutyric acid-co-3-hydroxyvaleric acid) grafted with chitosan and chitooligosaccharide after immobilized with hyaluronic acid.* Biomaterials, 2003. **24**(16): p. 2685-93.
22. Callahan, L.N., et al., *Dextran sulfate blocks antibody binding to the principal neutralizing domain of human immunodeficiency virus type 1 without interfering with gp120-CD4 interactions.* J. Virol., 1991. **65**(3): p. 1543-1550.
23. Harrison, J.H., *Dextran as a plasma substitute with plasma volume and excretion studies on control patients.* Ann Surg, 1954. **139**(2): p. 137-42.
24. de Jong, S.J., et al., *Biodegradable hydrogels based on stereocomplex formation between lactic acid oligomers grafted to dextran.* J Control Release, 2001. **72**(1-3): p. 47-56.
25. Hennink, W.E., et al., *Biodegradable dextran hydrogels crosslinked by stereocomplex formation for the controlled release of pharmaceutical proteins.* Int J Pharm, 2004. **277**(1-2): p. 99-104.
26. Kim, B.S. and D.J. Mooney, *Development of biocompatible synthetic extracellular matrices for tissue engineering.* Trends Biotechnol, 1998. **16**(5): p. 224-30.
27. Silva, E.A. and D.J. Mooney, *Synthetic extracellular matrices for tissue engineering and regeneration.* Curr Top Dev Biol, 2004. **64**: p. 181-205.
28. Hutmacher, D.W., et al., *Mechanical properties and cell cultural response of polycaprolactone scaffolds designed and fabricated via fused deposition modeling.* J Biomed Mater Res, 2001. **55**(2): p. 203-16.
29. Lowry, K.J., et al., *Polycaprolactone/glass bioabsorbable implant in a rabbit humerus fracture model.* J Biomed Mater Res, 1997. **36**(4): p. 536-41.
30. Kulkarni, R.K., et al., *Biodegradable poly(lactic acid) polymers.* J Biomed Mater Res, 1971. **5**(3): p. 169-81.
31. K.C. Dee, A.D.P., R. Bizios, *An introduction to tissue-biomaterial interactions.* John Wiley & Sons, Hoboken, 2002.
32. Engelberg, I. and J. Kohn, *Physico-mechanical properties of degradable polymers used in medical applications: a comparative study.* Biomaterials, 1991. **12**(3): p. 292-304.
33. Averous, L., et al., *Properties of thermoplastic blends: starch-polycaprolactone.* Polymer, 2000. **41**(11): p. 4157-4167.
34. Lee, J.W., et al., *Importance of integrin beta1-mediated cell adhesion on biodegradable polymers under serum depletion in mesenchymal stem cells and chondrocytes.* Biomaterials, 2004. **25**(10): p. 1901-9.
35. Massia, S.P. and J.A. Hubbell, *Covalently attached GRGD on polymer surfaces promotes biospecific adhesion of mammalian cells.* Ann N Y Acad Sci, 1990. **589**: p. 261-70.
36. Zhang, H., C.Y. Lin, and S.J. Hollister, *The interaction between bone marrow stromal cells and RGD-modified three-dimensional porous polycaprolactone scaffolds.* Biomaterials, 2009. **30**(25): p. 4063-9.
37. Karakecili, A., et al., *Relationship between the fibroblastic behaviour and surface properties of RGD-immobilized PCL membranes.* J Mater Sci Mater Med, 2007.

18(2): p. 317-9.
38. Hollister, S.J., *Scaffold Design and Manufacturing: From Concept to Clinic.* Advanced Materials, 2009. **21**(32-33): p. 3330-3342.
39. Harrison, N.M., et al., *Heterogeneous linear elastic trabecular bone modelling using micro-CT attenuation data and experimentally measured heterogeneous tissue properties.* J Biomech, 2008. **41**(11): p. 2589-96.
40. Kohles, S.S. and J.B. Roberts, *Linear poroelastic cancellous bone anisotropy: trabecular solid elastic and fluid transport properties.* J Biomech Eng, 2002. **124**(5): p. 521-6.
41. *Tissues and Organs*. Home ed. 2006, NJ: The Merck Manuals.
42. Weiss, J.A., J.C. Gardiner, and C. Bonifasi-Lista, *Ligament material behavior is nonlinear, viscoelastic and rate-independent under shear loading.* Journal of Biomechanics, 2002. **35**(7): p. 943-950.
43. Lieleg, O., et al., *Cytoskeletal Polymer Networks: Viscoelastic Properties are Determined by the Microscopic Interaction Potential of Cross-links.* Biophysical Journal, 2009. **96**(11): p. 4725-4732.
44. Sack, I., et al., *The impact of aging and gender on brain viscoelasticity.* NeuroImage, 2009. **46**(3): p. 652-657.
45. Farran, A.J.E., et al., *Effects of Matrix Composition, Microstructure, and Viscoelasticity on the Behaviors of Vocal Fold Fibroblasts Cultured in Three-Dimensional Hydrogel Networks.* Tissue Engineering Part A, 2009.
46. Fung, Y., *Elasticity of soft tissues in simple elongation.* Am J Physiol, 1967. **213**(6): p. 1532-1544.
47. Nekouzadeh, A., et al., *A simplified approach to quasi-linear viscoelastic modeling.* J Biomech, 2007. **40**(14): p. 3070-8.
48. Craiem, D., et al., *Fractional-order viscoelasticity applied to describe uniaxial stress relaxation of human arteries.* Phys Med Biol, 2008. **53**(17): p. 4543-54.
49. Boyce, B.L., et al., *Stress-controlled viscoelastic tensile response of bovine cornea.* J Biomech, 2007. **40**(11): p. 2367-76.
50. Defrate, L.E. and G. Li, *The prediction of stress-relaxation of ligaments and tendons using the quasi-linear viscoelastic model.* Biomech Model Mechanobiol, 2007. **6**(4): p. 245-51.
51. Swerup, C. and B. Rydqvist, *A mathematical model of the crustacean stretch receptor neuron. Biomechanics of the receptor muscle, mechanosensitive ion channels, and macrotransducer properties.* J Neurophysiol, 1996. **76**(4): p. 2211-2220.
52. Craiem, D.O. and R.L. Armentano. *Arterial viscoelasticity: a fractional derivative model*. in *Engineering in Medicine and Biology Society, 2006. EMBS '06. 28th Annual International Conference of the IEEE*. 2006.
53. Suki, B., A.L. Barabasi, and K.R. Lutchen, *Lung tissue viscoelasticity: a mathematical framework and its molecular basis.* J Appl Physiol, 1994. **76**(6): p. 2749-2759.
54. Tillman, J., A. Ullm, and S.V. Madihally, *Three-dimensional cell colonization in a sulfate rich environment.* Biomaterials, 2006. **27**(32): p. 5618-26.
55. Ghasemi-Mobarakeh, L., et al., *Electrospun poly(epsilon-caprolactone)/gelatin nanofibrous scaffolds for nerve tissue engineering.* Biomaterials, 2008. **29**(34): p.

4532-9.
56. Tillman, B.W., et al., *The in vivo stability of electrospun polycaprolactone-collagen scaffolds in vascular reconstruction.* Biomaterials, 2009. **30**(4): p. 583-8.
57. Prabhakaran, M.P., et al., *Electrospun biocomposite nanofibrous scaffolds for neural tissue engineering.* Tissue Eng Part A, 2008. **14**(11): p. 1787-97.
58. Lawrence, B.J., et al., *Multilayer composite scaffolds with mechanical properties similar to small intestinal submucosa.* J Biomed Mater Res A, 2009. **88**(3): p. 634-43.
59. Walboomers, X.F., et al., *Growth behavior of fibroblasts on microgrooved polystyrene.* Biomaterials, 1998. **19**(20): p. 1861-8.
60. Degirmenbasi, N., et al., *Surface patterning of poly(L-lactide) upon melt processing: in vitro culturing of fibroblasts and osteoblasts on surfaces ranging from highly crystalline with spherulitic protrusions to amorphous with nanoscale indentations.* J Biomed Mater Res A, 2009. **88**(1): p. 94-104.
61. Mirani, R., *Stress Relaxation Modeling Of Composite Porous Scaffolds*, in *Chemical Engineering*. 2009, Oklahoma State University: Stillwater.
62. Mirani, R.D., et al., *The stress relaxation characteristics of composite matrices etched to produce nanoscale surface features.* Biomaterials, 2009. **30**(5): p. 703-10.
63. Sarver, J.J., P.S. Robinson, and D.M. Elliott, *Methods for quasi-linear viscoelastic modeling of soft tissue: application to incremental stress-relaxation experiments.* J Biomech Eng, 2003. **125**(5): p. 754-8.

VITA

KORNKARN MAKORNKAEWKEYOON

Candidate for the Degree of

Master of Science

Thesis: POLYCAPROLACTONE MATRICES GENERATED IN AQUEOUS MEDIA: NATURAL POLYMERS IMMOBILIZATION AND STRESS RELAXATION BEHAVIOR

Major Field: Chemical Engineering

Biographical:

Personal Data: Born in Bangkok, Thailand on December 21, 1984

Education: Graduated from Assumption Convent School, Bangkok, Thailand in March 2003; received a Bachelor of Engineering degree in Chemical Engineering from Chulalongkorn University, Bangkok, Thailand in April 2007; Completed the requirements for the Master of Science degree with a major in Chemical Engineering at Oklahoma State University in May 2010.

Experience: Worked as an intern in PTT Chemical Public Company Limited from March – May 2006; currently employed by the Department of Chemical Engineering at Oklahoma State University as a graduate research assistant.

Name: KORNKARN MAKORNKAEWKEYOON Date of Degree: May 2010

Institution: Oklahoma State University Location: Stillwater, Oklahoma

Title of Study: POLYCAPROLACTONE MATRICES GENERATED IN AQUEOUS MEDIA: NATURAL POLYMERS IMMOBILIZATION AND STRESS RELAXATION BEHAVIOR

Pages in Study: 64 Candidate for the Degree of Master of Science

Major Field: Chemical Engineering

Scope and Method of Study:

This study determined the possibility of immobilizing natural polymers onto self-assembled polycaprolactone (PCL) matrices and its effect on tensile properties of the PCL matrix. The stress relaxation behavior of self-assembled PCL was also investigated by studying the effect of strain rate and natural polymers immobilization. Pseudo-component model was was tested with the experimental data using combinations of pseudo-components in order to find the best fit and gain better understanding of the stress relaxation behavior of self-assembled PCL.

Findings and Conclusions:

The immobilization of natural polymers onto self-assembled PCL matrices was confirmed but the attachment of chitosan porous structure was too weak to be used for tissue regeneration. The immobilized matrices had higher elastic modulus than those of self assembled PCL matrices in both wet and dry conditions. The effect of strain rate, at least in the range used in the experiment (0% s^{-1} -3% s^{-1}) was statistically insignificant on stress relaxation behavior. No statistically significant difference in the stress relaxation behavior was observed after the immobilization of natural matrixes. The proposed reform and retain pseudo-component concepts did not provide the best fit, but all forms of the pseudo-component model showed good fits in multiple stages. This is an improvement over traditional QLV model ability, and shows promise for being the modeling approach suitable for describing viscoelastic behavior of biomaterials.

ADVISER'S APPROVAL: Dr. Sundararajan V. Madihally